Magnetically Responsive Polymer Colloids of Cobalt Ferrites Nanoparticles for Theranostic Applications

By

Nada Saleh

School of Chemical and Materials Engineering (SCME)

National University of Sciences and Technology (NUST)

2018

Magnetically Responsive Polymer Colloids of Cobalt Ferrites Nanoparticles for Theranostic Applications

Nada Saleh

Registration Number: 00000172311

This thesis is submitted as a partial fulfillment of the requirements for the degree of

MS Material Science and Surface Engineering

Supervisor: Dr. Nasir M. Ahmad

School of Chemical and Materials Engineering (SCME)

National University of Sciences and Technology (NUST) H-12

Islamabad, Pakistan

August, 2018

Dedication page

No work can reach success but with Allah's will,

I dedicate my work to my parents,

Whose prayers and encouragement supports me to achieve success in fulfillment of my task.

Acknowledgement

Abstract

There are extensive research efforts being carried out to develop next generation theranostic smart materials and their employment for elaborative biomedical applications including combination of both therapy and diagnostics. Enhancement in the functionalities of the colloids and their application in biomedical theranostic is latest area of interest. In view of above, present project aims to develop the magnetically responsive polymers colloids for theranostic applications. Magnetic nanoparticles of $CoFe_2O_4$ were synthesized using co-precipitation method by iron nitrate (Fe $(NO_3)_3$.$9H_2O$) and cobalt nitrite (CO $(NO_3)_2$.$6H_2O$) salts in NaOH as precipitating agent. Particles were acid treated and characterized. Magnetically responsive polymer colloids were also synthesized by single emulsion solvent evaporation technique. Organic phase contained Methotrexate (MTX) drug, Eudagrit E100 and $CoFe_2O_4$ in ethanol whereas, aqueous phase contained polysorbate in deionized water. Optimization technique was employed to get stable emulsion by varying concentration of Methotrexate, Eudagrit and $CoFe_2O_4$, total of 40 formulations, 20 each HNO_3 treated untreated $CoFe_2O_4$, were produced at sonication amplitude of 60% at 20 kHz. After centrifugation at 13,000 rpm and lypholization at -76 ^{o}C at 0.014 mbar, the prepared magnetic polymer colloids were thoroughly characterized for their sizes, sizes distribution, surface charges, magnetic properties, morphology and composition. To determine the therapeutic potential of the prepared emulsion drug release experiment was carried out. Total encapsulated MTX content in the optimized emulsion was 55%. Dissolution was observed for up to 48 hours and total 8 samples were collected at fixed time interval for nanoparticles of iron cobalt coated eudagrit e 100 polymers which corresponds to 90 % drug release. In order to determine kinetics of the drug release different models such as zero order, first order, Higuchi, Hixen Crowell and korsemeyer Peppas models. Best fit model has been chosen on the basis of correlation coefficient (R^2) i.e. Hixon Crowell model. The developed project has significant potential in biomedical diagnostic and therapeutic applications in future

Table of content

List of Tables

List of Figures

1   Chapter 1: Introduction and Background

1.1   Introduction:

Smart polymers are materials that change their color or transparency, conductivity, permeability to water and shape when they are exposed to certain change in environment, temperature, PH, humidity, varying electrical and magnetic fields or any other trigger. They have great application in biomedical engineering, for instance certain polymer undergoes conformational changes if surrounding pH changes. The response of such polymers is not linear which makes them very unique. With difference in slight change in environment polymer changes its structure and properties. On microscopic level each individual monomer of smart polymer is weak, but their combine effect creates considerable force for biological reaction to happen. Magnetically responsive polymer colloids have wide application in the field of bio imaging. Theranostic application uses set of strategies together, i.e. targeting, imaging and therapy. Nano-particles that are magnetic in nature have gained a lot of attention in this area due to their compelling properties. Worldwide Rate of cancer is ever increasing many techniques has been developed in this regard. Approximately 2 million cases of cancer are anticipated to be identified by 2018 worldwide and the rate is ever increasing, according to International Cancer Society [1]. As a solution to this problem, nanoparticles are functionalized with different polymers and therapeutic agents and used for theranostic applications. Chemotherapy and other techniques are widely known for cancer treatments, but they affect healthy tissues in the human body. In order to control the damage caused by chemotherapies number of drug delivery systems has been designed especially a lot of work in the area of Nano medicines is been done in recent years [2][3][4]. Theranostic application implies that management of the disease doesn't only include treatment and the diagnoses, it also take account of observation of the drug distribution and therapeutic competence [5]. Also, it is Non- invasive imaging: due to which it is less excruciating. This project aims to develop emulsion by adjusting variables and parameters that affect its stability and performance. Secondary objective is validation of drug release profile in accordance with kinetic models. Super paramagnetic nanoparticles has many applications [6]

1. Bio distribution and target site accumulation via Noninvasive valuation and Monitoring of Drug release

2. Triggered drug release for improvement of therapeutic effectiveness and Therapeutic response Calculation
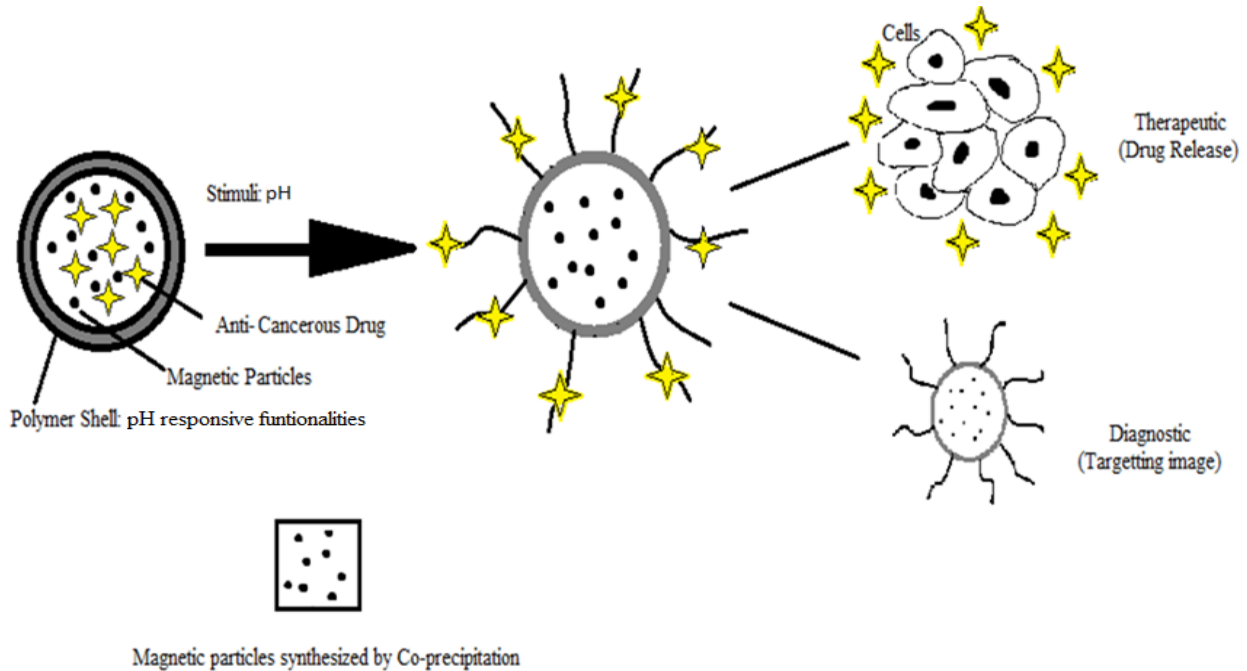
Fig 1.1 Graphical representation of MBTN

Representing stimuli responsive function to diagnose via imaging and therapeutic via drug release

1.2   Synthesis of magnetic nanoparticles:

Nanoparticles are manufactured by following techniques:

1. Co-precipitation method: It is very simplistic technique, in which metallic components from salt solution are reduced by addition of NaOH under ambient conditions. Properties such as size, shape and composition of the nanoparticles are governed by nature of salt which is employed for the synthesis.
2. Hydrothermal synthesis: In this technique nanoparticles area synthesized under high pressure and temperature. At the interfaces of three phases where phase transfer and separation mechanism is occurring. Temperature varies from 130 to 250 ^{o}C and pressure

reaches up to 4MPa. After completion of reaction Cooling to room temperature and washing is done.

3. Micro emulsion: It is a technique which consists of three phases polar (aqueous), nonpolar (organic) and surfactant. The role of the surfactant is to combine the polar phase with the non-polar phase. Polar phase is mixed with the in organic salt and precipitating agent. This aqueous solution is than added into organic phase drop wise into the organic phase, where nano-droplets of aqueous acts as catalyst and precipitates out nanoparticles.

4. Thermal decomposition: This technique involves decomposition of the organometallic compound at very temperature. After that oxidation is done in the presence of stabilizing surfactants and organic solvents with high boiling temperature. High temperature and operation complications results into highly Mono-disperse magnetic nano particles.

5. Sol-gel: In this technique hydrolysis and poly condensation reactions of the metallic precursors, metals or metalloid elements surrounded by different reactive ligands to form a system called 'sol'. Highly mono disperses and large sized nanoparticles are synthesized with this technique.

1.3   Classes of Magnetic materials

Magnetic materials are classified into five categories depending on their magnetic properties. [55]

a. **Ferromagnetic:** These materials have overall magnetic moments and hence show a large positive χ which indicates that the magnetic dipoles strongly align in the direction of applied field. In ferromagnetic materials magnetization perseveres even after the removal of the external field.

b. **Ferrimagnetic:** In Ferrimagnetic materials magnetization is stronger in one sub lattice as compared to the other, due to which magnetization remains even after removal of the external field. The number of spins in each sub-lattice is opposite and unequal.

c. **Anti-ferromagnetic:** The magnetization of the two opposite sub lattices is equal in magnitude in this case (i.e. the number of spins in each sub-lattice is opposite and equal).

As a result, the magnetization of one cancels out that of the other and there in no net magnetization in the material.

d. **Paramagnetic:** Atoms of paramagnetic only shows magnetic properties in the presence of the external magnetic field. As the magnetic field is removed magnetization vanishes. Atom and molecules are randomly aligned and they have net magnetic momentum. But due to heat some atoms remain disoriented.

Magnetite nanoparticles are paramagnetic at room temperature because of their small size.

e. **Diamagnetic:** these materials do not have any dipole because of filled electron shells. They have negative dipole because they tend to cancel the applied magnetic field.

Type	Alignment
Paramagnet	↓↘↓↖↓↗↓
Ferromagnet	↑↑↑↑↑↑
Anti-Ferromagnet	↑↓↑↓↑↓↑
Ferrimagnet	↑↓↑↓↑↓↑
Diamagnet	↑↑↓↓↓↑↑

Table. 1-1 Classes of magnetic materials

1.4 Magnetic behavior of Nano particles:

Nanoparticles have tendency to create a self-magnetic field when they are placed in external magnetic field. Angular momentum is of three types:

1. Orbital angular are the permanent orbital angular magnetic dipole moments.
2. Electron spin angular momentum is due to electron spin magnetic moments.
3. Nuclear spin angular moments are due to nuclear magnetic moments.

1.5 Structures of ferrites:

The general formula for spinel ferrites is AB_2O_4. Ferrite oxide chemical formula has M^{2+} Fe^{3+} O_4^{2-} chemical formula, where M^{2+} is any divalent metallic ion. Ferrites have tendency to crystallize in the form of cubic structure, where ferrite molecules are present that each corner of the unit cell. Usually cations are located at tetrahedral and octahedral locations while anions of oxygen are located at FCC positions. On the basis of scattering of cations on A and B sub lattices varying magnetic properties are exhibited by spinel ferrites such as: ferromagnetic,

antiferromagnetic and paramagnetic. In this area huge amount or research is been carried out of spinel ferrites due to their potential application for example, magnetite (FE_3O_4) derived compounds like $Fe_{3-x}M_xO_4$, where M is magnetic or non-magnetic elements such as Co, Mn, Zn, etc. Cobalt exhibits anisotropic properties due to which s has potential application as chemical sensors [7] [8][9][10][11]. Hence there are total eight atoms in the ferrite unit cell i.e. 8 are M^{2+}, 16 are Fe^+ and 32 O^{-2}. Oxygen ions in the structure constitute of a close packed face centered cubic structures. Therefore, 4 O^{-2} ions there are 2 octahedral sites and one tetrahedral site. The 6 O^{-2} surrounds octahedral sites and 4 O^{-2} ions surround one tetrahedral. Whereas the total number of octahedral sites are double, than tetrahedral sites because metal ions are dispersed over tetrahedral and octahedral sites.

Following are the 2 types of ferrite structures:

1. Regular spinel
2. Inverse spinel

1.5.1 Regular spinel

in a unit cell, there are 8 tetrahedral (8 A) sites out of which one is occupied by divalent metal ion, and 16 octahedral (16B) out of which 1 site is taken by trivalent metal ion.
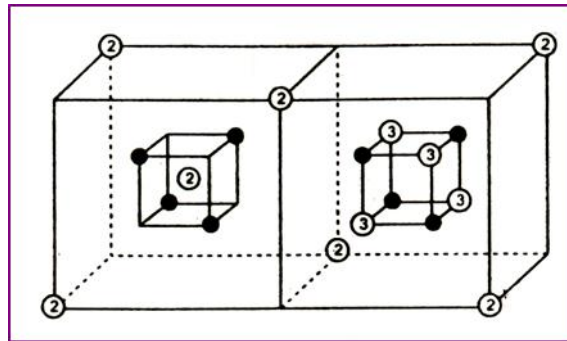
Fig.1.2 Schematic of Cobalt Ferrite [56]

1.5.2 Inverse spinel

In this type half of the B sites (8sites) are occupied by divalent metal ions and the remaining half of the B sites (8 sites) and all the A sites are occupied by the trivalent metal ions, as shown in Fig.
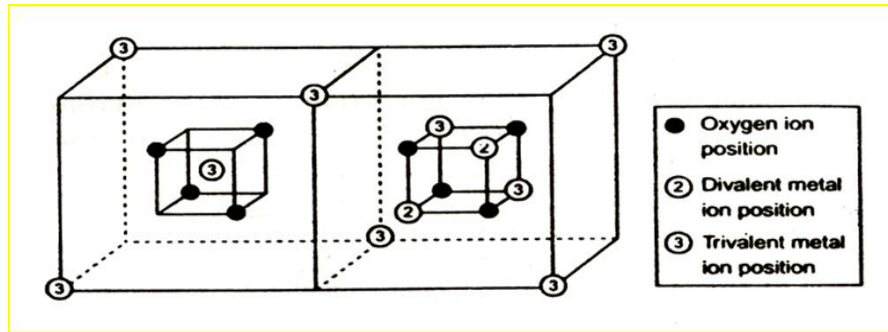
Fig.1.3 Schematic of ferrous ferrite molecule [56]

Formation of drug loaded targeted nanoparticles using nano precipitation method and single emulsion for cancer treatment:

Therapeutic DDS controls targeted supply of the drug to the tumor sites and limits the interaction of drug with the healthy tissues. Chemotherapy results in damage of the healthy cells by inhibiting processes of cell division in the body by controlling the DNA synthesis of highly dividing cells.

There are three core methods of creating Nano carriers for drug delivery [11]

1. Nano-precipitation: In this method organic phase is mixed in the aqueous phase those results into spontaneous precipitation of the nanoparticles.

2. Single emulsion: In single emulsion water or aqueous phase is added by drop wise technique into organic phase or vice versa. The nanoparticles remain homogenously suspended into the formulation

3. Double emulsion: in this technique single emulsion is added into the organic or aqueous phase depending on the outer most layers. Forming three layers i.e. Oil/Water/oil or vice versa.

The ideal nanoparticle for theranostic application has many advantageous properties [12]:

1. Tendency for targeted tumor accumulation
2. Detection of tumor at early stage along with supply of anti-cancer drugs
3. They are Biocompatibility and bio degradable

1.6 Encapsulation via single emulsion- desolvation technique:

Samples holding medicine and nanoparticles were synthesized using simple emulsion evaporation; this technique involves simple emulsion formulation followed by evaporation of the solvents that results into the particle formation. Organic phase (labeled as mixture A) contained Methotrexate, Eudagrit and $CoFe_2O_4$ magnetic nanoparticles were mixed in ethanol. Aqueous phase (labeled as mixture B) was formed after the formation of organic phase by mixing polysorbate in deionized water. Organic phase was inserted drop wise in the liquid phase to form emulsion and sonicated for few minutes [59]. Following are the parameters that control the particles Phase ratio of Organic phase/water:

1. Nature and concentration of Surfactant

2. Sonication Rate

3. Amount of Polymer

4. Amount of Cobalt ferrite nano particles

5. Amount of organic solvent

Following are the properties of the chemicals that are used for emulsion formulation:

Eudragit E100

1. Cationic copolymer based on dimethylaminoethyl methacrylate

2. Transition temperature (48 °C).

3. PH sensitive dissolves when pH is greater than 7.

4. Eudragit E 100 has been used in nanoparticles and floating drug delivery system

5. Depending on the functional groups used in the polymer, Eudragit formulations can be precisely tuned to the type of drug release – immediate, delayed or sustained – desired by the formulator.
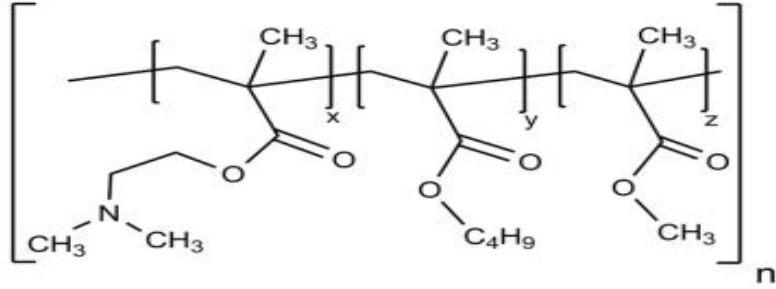
Fig 1.4 Structure of Eudagrit E 100

Tween 80:

1. nonionic compound with chemical nomenclature of is Polyoxyethylene (20) sorbitan monooleate or (x)-sorbitan mono-9-octadecenoate poly(oxy-1,2-ethanediyl)

2. This synthetic compound is water soluble, yellow in color and viscous.

3. It is often used in foods and cosmetics

4. It is derived from polyethoxylated sorbitan and oleic acid.

5. It is mostly used as emulsifier to stabilize aqueous formulations of medications.

$w+x+y+z=20$
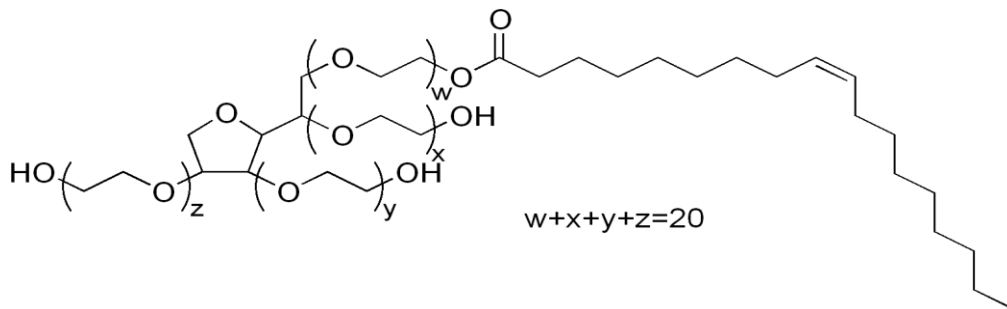
Fig 1.5 Structure of Tween 80

Methotrexate (MTX) $C_{20}H_{22}N_8O_5$

1. Its formula name is N-[4-[[2,4-diamino-6-pteridinyl)methyl]methylamino]benzoy]-L-glutamic acid.

2. It is chemotherapic agent which is mainly used for the treatment of cancer.

3. It has high efficacy, it is available as generic medicine.

4. It is highly safe medicine.

5. It is supplied has crystalline solid, its solution is made by dissolving it dimethyl formamide or DMSO.

6. It has ph of 7.2 and remains stable for more than 2 years.
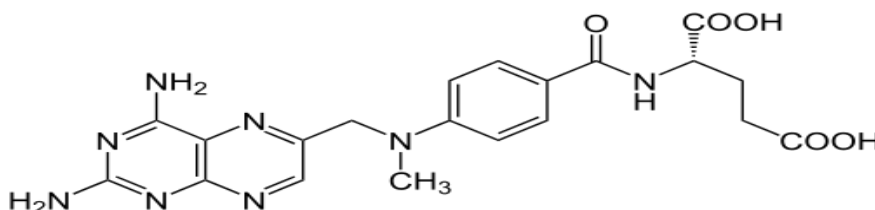
Fig 1.6 Structure of Methotrexate (MTX)

Ethanol C_2H_5OH

1. It is a chemical compound with many chemical names like ethyl alcohol, ethylol, ethyl hydrate, methylcarbinol and so on.

2. Its medical application is antiseptis and disinfectant.

3. It has no color with faint characteristic smell.

4. It's highly flammable and volatile.

5. Its ph is neutral and produced by fermentation
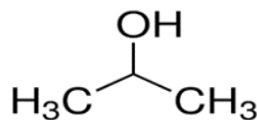
Fig .1.7 Structure of Ethanol

9

2 Chapter 2: Literature review

A lot of research has been carried out in the field of magnetic based theranostic nanoparticles (MBTN) systems for biomedical applications. Magnetic particles have gained a lot of popularity in this region due to their ability to be used under MRI. In order to increase efficiency nanoparticles are decorated with variable materials to increase their biocompatibility to transport therapeutic loads, to put imaging agents in polymeric shell and deliver functional groups for conjugation of biomolecules that offer receptor mediated targeting of the disease. Recently, theranostic applications have attained lot of attention due to their diagnostic and therapeutic ability. In this area review work by Aniket S. and Jyothi U [13] showed comparison between different core, shells, imaging, therapeutic and targeting agents and their applications. The results showed that Magnetic particles have diverse functionality for instance site explicit magnetic targeting, Negative contrast agents for MRI, Hyperthermia treatment with changing magnetic fields, Controlled drug delivery under magnetic field Due to above mentioned application MNP has wide scope in theranostic applications. Usually as iron, cobalt, or their oxide that are ferromagnetic elements are used. Such elements can be easily flushed out of the body in the form of iron and oxygen.

Therapeutic modalities and better imaging in management and control of cancer has become leading research are due to increased rate of cancer. Magnetic based therapeutic Nano particles (MBTN) have multi-function due to their combined magnetic and therapeutic properties. There are two ways to attach drug with nanoparticles that is either they are encapsulated or it is attached with the surface, for instance when MNP coated and treated with MTX and Chlorotoxin-conjugated were targeted at tumor cell, there was decreased in the survival rate of the cancer cells [14] Moreover when methotrexate loaded nanoparticles were induced in mice with tumor decrease in the size of tumor was observed within 19 days [15].

Theranostic system was developed for intravenous administration, this study aimed at the manufacturing of colloidal delivery system by using solid lipid nanoparticles (SLN). The SLN contained medicine methotrexate and iron oxide super-paramagnetic particles. This formulation was designed for very common autoimmune disease (Rheumatoid Arthritis (RA)). RA infected macrophages were targeted by anti-body CD64 that were attached to the surface of SLN. By

organic solvent free emulsification-sonication method total eight formulations were formed. Stability of the formulation was up to one month. TEM was conducted in order to analyze the morphology and FT-IR confirmed the presence of MTX and SLN. Cytotoxicity of Formulation was proved to be bio-compatible by performing in-vitro test on THP-1 cells. [16]

Magnetic nanoparticles have been employed for treatment of cancer, application of magnetic nanoparticles for their application in bio medical field; they need to fulfill certain criteria. A lot of research has been carried out in this regard, and different techniques are designed. Magnetic nanoparticles are usually manufactured by co precipitation method, hydrothermal synthesis, micro emulsion, thermal decomposition and sol-gel. Later encapsulation of the magnetic particles in the polymer or any organic phase is carried out by different techniques such as, Nano precipitation, simple emulsion, double emulsion, and layer by layer process. Magnetic particles due to their interaction with external magnetic field and transverse radio frequency pulse. When these ways strike the proton exists and return back by relaxation phenomenon, this relaxation time is different for different organs and tumors, due to which contrast is generated. As the result of these unique properties they can be engaged for drug distribution and hyperthermia. In hyperthermia magnetic particles are delivered to the site and excited resulting into very high localized temperature that destroys the cancer cells. [17]

The review work done by Nathalie. S and Fabienne. D [18] focused on different advancements techniques to address major issue of lack of selectivity in cancer therapies. Three main strategies are passive targeting; active targeting and stimuli mediated targeting. In this regard nanoparticles that possess theranostic application have proved a great leap in personalized therapy. Comparison was made between different contrast agents that are currently used for MRI. The review aimed to study the super paramagnetic iron oxide theranostic that have recently emerged. The work was divided into three sections in first section personalized therapies as biomedical application is discussed. In this section it was highlights that fro personalized treatment patients should be pre-selected on the basis of MRI results, if the tumor size is sufficient than treatment must be started and properly monitored within 1 to 3 cycles of treatments[19] .then different contrast agents were compared that are currently used and discussed. Results of comparison showed that SPIO can be employed for TDD, drug can either be covalently attached or trapped

in the polymer depending on the synthesis technique .in last section recent advancements are highlighted.

In this regard comparison was made between past five years advances for Cancer Applications on Distantly Activated Nano-Theranostics. Different distant activating tools were covered namely photodynamic, photo triggered chemotherapeutic release, ultrasound, electro-thermal, magneto-thermal, X-ray, photo thermal and RF therapies along with the various nanoparticles that are used employed with each method. Photosensitizer (PS) are non-toxic agent that are used in Photodynamic therapy (PDT). Light is irradiated by photosensitizers that forms active oxygen specie which results in the destruction of tumor cells at targeted area. [20] Novel nano units employed for PDT contain up converted nanoparticles [21-25, 26-31]. Optical imaging and other numerous Imaging modalities can be employed for the Light-sensitive diverse functionality nanoparticles to trace cancer cells in patients [32]. Photo-thermal therapy uses unremitting lasers that are either in the form of wave or pulsed to expose cancer cells by visible or near infra-red light electromagnetic radiation. This results in localized intensification in temperature ranging between 45-300 ^{0}C that causes demise of cells by converting laser energy to heat [33]. Ultrasound has wide application in medicine for a diversity of diagnostic and remedial purposes because it's non-invasive and may be absorbed at depth in soft tissue. It was suggested as a technique for activating drug distribution by Langer and co-workers in 1989 [34]. Lately, ultrasound has been sightseen as revenue of using exterior controller in drug distribution from biomaterials for pulsatile discharge. [35]. Electrical signals are outstanding distant activators that are employed for theranostic applications because they are easy to create and regulate. Conducting polymers were used in electrical delivery systems in which electrical stimuli were used to trigger the discharge of payloads [36], [37], [38]. Similarly X-rays is forms active oxygen specie which results in the destruction of tumor cells at targeted area, like in photodynamic therapy. Photosensitizer conjugated with CeF_3 nanoparticles were employed for release of a $[O]^-$ species upon X-ray irradiation of 8 keV. Radiofrequency activated hyperthermia is one more prevalent distantly activated remedy method. Another research Elsherbini et al. found out that by employing gold-coated magnetic Nano composites to induce hyperthermia in carcinoma in mice, more than half of the tumors vanished entirely under exposure of light or radiofrequency, [39][40].

Reverse micro emulsion method was used for the manufacturing of PEG- modified nanoparticles. Super paramagnetic behavior was shown by Nanoparticles with core of magnet and shell of polymer.

Transmission electron microscopy (TEM), IR spectroscopy, atomic force microscopy (AFM), vibrating sample magnetometer (VSM), and ultraviolet/visible spectroscopy were carried out to evaluate the characteristics properties of the emulsion. Cytotoxicity profile of the emulsion showed that the emulsion is safe and nontoxic. Reverse microemulsion was manufactured from inverse micro emulsion approach, in which reverse micelles were connected with the hydrophilic compounds, as inverse micelles have aqueous inner core. Benefit of using reverse micelle is that sizes of the nanoparticle can be fixed. [41] For medical applications physical properties like size, surface chemistry and charge is very important because it not only effects the blood circulation but also the bioavailability of the particles within body. [42]

Particle size is of great importance as the particles that are <10 nm are excreted by the renal clearance in extravasations. Whereas elements that are >200 nm get stuck in spleen as a result of the mechanical separation. Particles size within range of 10-100 nm is optimal for this type of applications. [43]

Dual imaging enhances detection of cancer in its early stages. For this purpose nano-emulsion was formed with cobalt ferrite nano particles with drug of lecithin, for photo acoustic and MRI [44]. Lipoid lecithin and water of Milli-Q rendering to a former reported work. [57] Soy-bean was mixed with Lipoid to form organic phase. The organic phase was blended by alternating high speed blender. Cobalt-iron oxide Nano-cubes were added into toluene solution, this mixture solvent was evaporated after adding the mixture in it. In vitro conditions nanoparticles were responsive in both photo acoustic and MRI. In murine melanoma xenograft model clear time dependent accumulation of the tissues of tumor were shown via photo acoustic studies. Emulsion can be employed as T_2 weighted image contrast agent as it has higher values of the r_2/r_1 ratio ranging from 45 to 85 are exhibited by Oil/Water emulsion on the basis of external magnetic field. Also, feasibility and cellular acceptance studies showed no toxicity on the fibroblast. Due to lipophilic properties, the nanocarrier were embedded in hydrophobic surfactant coated iron cobalt oxide nanotubes. Emulsion size was 165nm, which is sufficiently large to lower extravasation in healthy tissues and well below 200m. [45] Another research of iron cobalt

13

nanoparticles when incubated for 1μM for 72 hours with mouse fibroblast activated repair mechanism and the defensive cellular pathways. [46]

Nanoparticles of $CoFe_2O_4$ with therapeutic and optical properties of size 35-45 nm was synthesized using co-precipitation method. Solution of water with Ethyl-Dichloromide and N-hydroxysuccinide was formed; further solution was mechanically agitated for 2 hours in dark after addition of methotrexate. Later dispersion was kept in dark for 10 hours at ambient conditions. Then the particles separated by magnetic separator and washed thoroughly for in vitro studies after making buffer solution in phosphate. Concurrently 2 samples were also prepared, with conjugating RITC ($CoFe_2O_4$-FA-MTX), 2) and without conjugating FA and RITC ($CoFe_2O_4$-MTX) following the same procedure. Particles showed decent solubility both in zeta potential and hydrodynamic size in physiological aqueous dispersion. Toxicity and internalization of Nano-carriers were estimated on folate receptor overexpressed HeLa cells. Methotrexate and doxorubicin were attached to the surface of nanoparticles by following simple organic reaction by amine groups. Nano agents with drug resulted into elevated cytotoxicity and induce apoptosis. [65]

Nanoparticles of $CoFe_2O_4$ have excellent chemical stability due to first order crystalline anisotropy constant, it has many application due to which it is very important to control the particle size. Different size of nanoparticles of Cobalt Ferrite were formed by university of Puerto Rico [64], in which particle size was controlled by flow rate of the reactant in the solution. Particles were aid treated by adding Nitric acid in fixed amount of cobalt particles and allowing them to react for 30 minutes followed by washing and drying. Results obtained from VSM showed that acid treated particles showed Coercivity. Analysis results from XRD and FTIR showed that Coercivity increased, and ferrite formation started after 5minutes and M-H measurements showed that particle size influenced the magnetic properties.

There are many functional properties of the magnetic particles that make them good candidate for biomedical application, such as contrast agents. They can be used as targeted drug deliver due to their response to the external medical field. Magnetic nanoparticles were manufactured with general co precipitation method. Series of chemical reaction were carried out in order to from the contrast agent for biomedical application, firstly Fe^{2+} ions were investigated, and first

stabilizer was succinic anhydride which was employed to combine polymers, i.e. polyethylene glycol and palmitoylated Polyethylene glycol-grafted Chitosan (Cs-PEG-PA). Structure, magnetic properties, size and composition of the magnetic particles were observed with X-ray diffraction (XRD) and particle size analysis (PSA), Fourier transform infrared spectroscopy (FTIR) and vibrating sample magnetometer (VSM). Methotrexate was incorporated into surface modified nanoparticles. Reaction with sulphuric acid was carried out in order to react it with PEG. The carboxylic acid of MNPs' reacted to amine groups of Chitosan groups through the Ethyl-Dichloromide and N-hydroxysuccinide facilitated reaction, as a result high drug encapsulation efficiency at certain magnetization value was obtained. After 72 h the in-vitro release pattern was studied, showing only 6% at physiological environment (pH = 7.4) and 25% in tumor tissue environment (pH=5.4). on the basis of findings, this can be used as novel pH sensitive drug release for targeting cancer cells. Similarly pH-sensitive coated manganese ferrite nanoparticles were developed for delivery of methotrexate with Pegylated and amphiphilic Chitosan. [58]

Ferromagnetic nature of iron cobalt particles are proved by [49] in which mechanical alloying and subsequent annealing of iron cobalt was performed to obtained desired structural phase stability and magnetic properties of Co_2FeO_4 spinel ferrite oxide. Particle sized varied from 25nm to 45nm. XRD spectrum, SEM, along with EDAX spectrum and magnetic measurements were performed to found out phase separation of samples. The study indicated the ferromagnetic nature of $CoFe_2O_4$. Additional support to the results was provided by observation of mixed ferromagnetic phases at two different Curie temperature.

Cobalt ferrite ($CoFe_2O_4$) has many excellent chemical properties such as, excellent mechanical hardness, noble chemical stability with large affirmative 1st order crystalline anisotropy constant, however these properties are constrained by particle size distribution. The tendency to control particle size is very important which can be controlled by controlling oversaturation conditions. The main factors that contribute in final size of the cobalt particle is feeding flow rate of the reactant solutions. Improved co-precipitation method was employed for the synthesis of Nanoparticles, and different sized nano particles of cobalt ferrite were synthesis by varying flow rate ranging from 1-10 mL/min. Results showed that by controlling the flow rate of the solvent

growth of the crystal was promoted. Sample with flow-rate of 1mL/min showed least development of the ferrite, whereas FT-IR spectra for 10 mL/min exhibited clear trend. [50]

Thin films of Nano ferrites were employed as contrast agent for magnetically responsive engineered thin films. The work has huge scope for future lab on chip diagnosis. The application of magnetically responsive engineered Nano ferrites in MRI has emerged as new area. In human body they are used for labelling and tracking. Gandollium ion or super paramagnetic iron oxide ions both have their merits and demerits on the basis of T1 and T2 weighted imaging enhancement capabilities. Self-assembled multi thin layer of $NiFe_2O_4$ was manufactured by layer by layer method. By dipping alternatively glass micro slide in chitosan solution. By application of this procedure multilayer as well as single layer of the films can be obtained. Characterization of the film revealed that this study should be used as general protocol for different kind of imaging.[51]

Similarly, hybrid of magnetic nano particles of iron oxide was made with polycaprolactone. Nano particles of iron oxide were manufactured using modified method of co-precipitation. Emulsion with polycaprolactone was prepared by double emulsion evaporation method. Aqueous media contained the nano particles of iron oxide that was added into the organic media containing polycaprolactone in DCM. Poly vinyl Alcohol was employed as surfactant. Comparison with the commercially available Gadolinium for contrast efficiency in MRI tests showed enhancement in MRI contrast of the prepared particles. [52]

Improvement in the functionalities of the colloids and their application in biomedical imaging is latest area of interest. In this regard comparison was made between different contrast agents (Gadolinium, Gd-BOPTA, Iron Oxide), there associated relaxation time and coated stimuli responsive polymer, and application. There is a lot of current research involving magnetic colloids that can be prepared by using various antibodies, peptides, drugs, ligands and protein. Also bio thin films have unlocked novel revenue of research in the area of MRI. Bio thin films are usually formed by layer by layer method. There are two types of contrast agent's i.e. positive and negative that is determined by their relaxation time. Colloids based on SPIO's decreases the T2 relaxation time, Gd and Mn based contrast agents decrease T1 relaxation time. Also, ultra-

small SPIO has the capability to induce changes in T1 and T2. The comparison revealed that colloids of super-paramagnetic iron oxide (SPIO) are very important for the next generation bio imaging. [53]

Submicron particles were developed and studied by K. Lima and Edgardo in their work on amino dextran polymer- functionalized reactive magnetic emulsions. In this research particles were synthesized by Aminodextran, which was obtained by chemical attachment of hexa-methylenediamine on oxidized dextran. Magnetic particles carried negative charged that were easily attached with positively charged aminodextran particles. The range of the AMD absorbed per gram of dried magnetic dispersion varied from 20 to 1280 mg. the AMD-coated particles were evaluated in zeta potential from 3 to 9 pH paralleled with the blank seed magnetic emulsion. The particles possessed noble potential for in vivo biomedical application, due to higher contrast capability matched to Gd in MRI. [54]

3   Chapter 3: Solution and Methodology

3.1   Materials

Eudagrit S100 (Evonik industries, Darmstadt, Germany), Iron nitrate Fe $(NO_3)_3.9H_2O$, Cobalt nitrate CO $(NO_3)_2 .6H_2O$), and Sodium Hydroxide NaOH (Merck, Emsure, 99% pure, Germany), Tween 80 (BDH supplies laboratory, England), Methotrexate (MTX) (specs), Ethanol (Sigma Aldrich Germany)

3.1.1   Apparatus and Equipment:

Magnetic Hot plate with stirrer (MSHO 1A 111, PCSIR, Islamabad, Pakistan), Furnace (Product of PCSIR, Pakistan, Muffle Furnace), Oven (MEmmer, Chemical MFG Corp), bath sonicator (ElmaSonic ultra sonication), probe sonicator (Vibra cell, Sonics), Measuring   balance   (PA 214C, Ohaus Corporation, USA) Rotary Evaporator (Hei-VAP, Heildph USA),Water Deionized water (Elgacan Cartridge C114, Electric heated Stainless Steel, China), pH meter (PHS 25CW, Bante instruments Chicago, USA) , pharmaceutical refrigerator (MPR-161D H, Panasonic, Japan), lyophilizer (Alpha 1-2 LD plus, Christ, Germany), centrifugation machine (Hermle labortechnikZ-206A, Germany)

Glassware: Beaker (1000 ml, 500ml, 100ml), 30 ml Glass vials, micro pipettes, rotary flask beaker (100 ml)

Other consumables: falcon tubes, eppendorf's tubes, pipette, Aluminum foil, Spatula, Butter paper, Teflon coated magnetic stirrer

3.2   Synthesis co-precipitation of Nano particles methodology:

Nanoparticles were manufactured by using co-precipitation method under ambient conditions. All the chemicals and reagents were of analytical grade and they were used without any further purification. Salts of iron and cobalt, that is Iron Nitrate (Fe $(NO_3)_3.9H_2O$) and Cobalt Nitrate (CO $(NO_3)_2 .6H_2O$) were taken in fixed amount with ratio 1:2 (Co: Fe), and mixed in distilled water to form ionic solution. Sodium hydroxide (NaOH) was used as precipitating agent for alkaline aqueous solution.

Equipment required:

1. Beaker (1000 ml and 500ml)
2. Magnetic Hot plate with stirrer
3. Furnace
4. Oven
5. Butter paper
6. Spatula

Chemical or material Used:

1. $Fe(NO_3)_3.9H_2O$
2. $CO(NO_3)_2 .6H_2O$
3. NaOH
4. Deionized water

Manufacturing of iron cobalt Nano particles by co precipitation:

Calculations were done by using following equation, Molecular weight of Fe $(NO_3)_3.9H_2O$ is 403.95 and CO $(NO_3)_2 .6H_2O$ is 291.04, that is inserted in formula:

Formula: $\frac{M_1 v_1}{n_1} = \frac{M_2 v_2}{n_2}$

Cobalt nitrite=

$$\frac{0.1 \times 291.04 \times 200}{1000} = 5.820 \, mg$$

Ferrite nitrite=

$$\frac{0.2 \times 403.95 \times 200}{1000} = 16.158 \, mg$$

1. Measure iron nitrate and cobalt nitrite according to the calculated amount and put butter paper on the measuring pan.
2. Add 400 ml deionized water to form ionic solutions. Simultaneously add ionic solutions in a beaker, followed by heat stirring till temperature reaches 90°C.
3. Than measure 15.9999 g/mol of NaOH and mix in 200ml of water.

4. Wait until solution of NaOH reach 70-80°C and ionic solution of salts of iron and cobalt to 90°C than mix the two.

5. When the two solutions achieved the required temperature, mix them and put them on heating. Following are conditions and specifications:

Temperature	370°C
Stirrer speed	4 RPM
Time	1 hour

Table 3-1 Reaction conditions

6. After an hour of heating 200ml was evaporated and temperature of the mixture was maintained at 80 ^{o}C.

7. Stop heating and continue to stir for about 30 minutes so that temperature drops to 25°C.

8. Allow the particles to settle.

9. Once the particle settle wash them by removing the excess water.

10. Now add deionized water to the remaining solution till 1000ml and allow it to settle again. Similarly repeat the processes until neutral pH is obtained.

11. After 5 washes pH was 8. After 8th wash pH was 7, as the pH drops to neutral particles takes more time to settle.

12. Once particle settle to the bottom of the beaker, remove the excess water and place it on hot plate at 75 ^{o}C.

13. Wait for the remaining water to evaporate, temperature must not rise above 100 ^{o}C.

Calcification:

After drying of the particle calcification was performed by placing the dried mixture in oven for 6 hours at 800 ^{o}C, later the mixture was taken out and crushed with high quality pastel and mortar to fine powder.

This fine powder was later placed in furnace for further complete drying at temperature 800 ^{o}C for time of 6 hours in furnace.

3.2.1 Properties:

Materials properties are very different on nanoscale as compared to the bulk scale. For instance electronic, chemical and optical properties on nano scale are different as compared

to the properties on the larger scale. Characterization of the nanoparticles was done with the help of the SEM, VSM and XRD that is discussed in chapter 4.

3.3 Acid Treatment:

Acid treatment of the particles was performed according to a work by university of Puerto Rico [64] to achieve stable dispersion of Nano-particles of cobalt ferrite in ethanol solution. Results of VSM and Zeta sizer showed that dispersion increased.

Method:

Following steps were followed:

1. Weigh 75mg of nano particles on balance
2. Use 20%v/v of nitric acid
3. Add in 75 ml of diluted nitric acid
4. Calculations:

Formula: $\frac{M_1}{V_1} = \frac{M_2}{V_2}$

5. Add nano particles in ethanol and treat for 30 minutes on sonicator at room temperature.
6. Let the particle settle, followed by washing.
7. After successive washing, dry them in oven for 4 hours.

VSM results showed that magnetic properties were not compromised and ethanol dispersion also increased.

3.4 Encapsulation via single emulsion- solvent evaporation technique:

Multiple Samples of varying concentration of the mixing elements was synthesized in order to find out the most suitable and stable ratio. There are different factors that determine the properties of the particles amongst which amount of polymer and surfactant is very important. Other actors are stirring rate, and Phase ratio of Organic phase/water.

Equipment/Apparatus:

1. Bath Sonicator
2. Measuring balance

3. Rotary Evaporator
4. Rotary flask beaker
5. 30 ml glass Viols(25)
6. Beaker 50 ml (10)
7. Pipette
8. Butter paper
9. Spatula

Chemical/Reagents:

1. Eudagrit 100
2. Tween 80
3. Magnetic particles of $CoFe_2O_4$(Treated/Untreated)
4. Methotrexate (MTX)
5. Ethanol
6. Deionized water

3.4.1 Parameter studied and adjusted:

Total of 40 formulations, 20 with untreated cobalt nanoparticles and 20 with treated cobalt iron nanoparticles were formulated by varying concentrations of ethanol, tween 80, magnetic particles of $CoFe_2O_4$ (Treated/Untreated) and Eudagrit E 100 polymer by keeping the stirring time and speed constant. Firstly emulsion concentrations parameter were varied and adjusted, then sonication ad stirring speed was studied and adjusted. On the basis of which best emulsion was selected, best emulsion is the one which easily redisperse on minute mechanical shaking. Following chart of the amount of materials that were used:

Codes	Solvent (ml)	Polymer (mg)	Surfactant (ml)	Nanoparticles (mg)	Drug (mg)	Characteristics of nanoemuslion
	Ethanol	(Eudagrit 100)	Tween 80	$Co_2Fe_4O_6$	MTX	Observations
E1	**4**	150	2	3	10	Heavy precipitation, No aggregates
E2	**6**	150	2	3	10	Very small precipitation, No aggregates
E3	**8**	150	2	3	10	Aggregates of $Co_2Fe_4O_6$
E4	**10**	150	2	3	10	Very small precipitation, No aggregates

E5	**12**	150	2	3	10	Very small precipitation, No aggregates
E6	6	**50**	2	3	10	Very heavy precipitation, No aggregates
E7	6	**100**	2	3	10	Slightly less precipitation, No aggregates
E8	6	**150**	2	3	10	Uniformly dispersed nanoparticles
E9	6	**200**	2	3	10	White threads of polymer were floating in emulsion
E 10	6	**250**	2	3	10	Floating and settling of excessive polymer
E 11	6	**300**	2	3	10	Floating and settling of excessive polymer
E 12	6	150	**0.5**	3	10	Heavy Aggregates of $Co_2Fe_4O_6$
E 13	6	150	**1**	3	10	Clumps of organic phase, Less foamy
E 14	6	150	**1.5**	3	10	Clumps of organic phase, Slightly more foamy
E 15	6	150	**2.5**	3	10	Homogenously stable
E 16	6	150	**3**	3	10	Stable, highly foamy due to excessive Tween
E 17	6	150	2	**1**	10	Very small precipitation
E 18	6	150	2	**1.5**	10	Small precipitation
E 19	6	150	2	**2**	10	Slightly high
E 20	6	150	2	**2.5**	10	High precipitation
Total	**130 ml**	**3150 mg**	**38.5 ml**	**55 mg**	**200 mg**	-

Table 3-3-2 Amount of reagents and chemicals for emulsion

3.5   Formulation of emulsion

Emulsion was formed by mixing organic phase in aqueous phase in two steps; firstly, organic phase was synthesized. Following are the steps that were carried for the manufacturing of the emulsion:

Preparation of Organic phase (Solution A):

1.   **Solution A1**: Fixed amount polymer Eudagrit 100 (i.e. for sample 1 is 100mg) was added in 2ml of ethanol and placed on bath sonicator for 15 minutes for complete dissolution and homogenous mixing.

2.   **Solution A2:** Then fixed amount magnetic nanoparticles (i.e. for sample 1 is 3mg) were added in 2ml of ethanol and placed on bath sonicator for 30 minutes for complete and homogenous mixing.

3.   **Solution A3**: Thirdly fixed amount Methotrexate (i.e. for sample 1 is 10 mg) were added in 2 ml of ethanol and placed on magnetic stirrer 15 for minutes for complete and homogenous mixing.

4.   Solution A1, A2 and A3 were then added one by one on glass beaker and stirred for 10 minutes without heating for complete mixing, this solution was labeled as solution A.

Preparation of Aqueous phase (Solution B):

5.   Aqueous phase was formed by mixing fixed amount of Surfactant (for instance for sample 1 is 2ml) Tween 80 in 20 ml of deionized water and stirred for 15 minutes, this solution was labeled as solution B.

Emulsion formation:

6.   Emulsion was formed by drop wise addition of organic phase (solution A) in aqueous phase (solution B)

7.   After complete addition of the mixture A into mixture B, it was allowed to sonicate for 2 minutes with 2 pulses on and one pulse off at amplitude of 60% at 20 kHz.

8.   Emulsion was then placed for 10 minutes without any stirring to settle.

9.   Formation was then poured into rotary flask and ethanol was evaporated. Rota Evaporator was set at 40°C and ethanol evaporated approximately within 15 minutes.

10.   Similar procedure was followed for the formulation of the rest of emulsions.

Observations

After the formulation of the emulsion samples on the basis of varying concentration parameter they were kept at ambient conditions in order to check there stability which was evaluated on basis of physical appearance and emulsion defects such as precipitation or thread formation of the polymer, settlement of the emulsion at the bottom of the viols, caking, creaming and phase separation. Following are the observations.

1. Emulsions with varying ethanol (sample 1 to 5) apparently affected the stability of the emulsion, amongst sample 2 showed the most stable emulsion with least settlement of the particles.

2. Emulsions with varying polymer (sample 6 to 11) impacted the emulsion properties, sample 6 and 7 that have minimum polymer had maximum settlement while sample 8 showed maximum stability, whereas samples with high quantity of polymer i.e. 9, 10, 11 had signs of excessive polymer, as thread like particles of crystalline polymer were floating in the emulsion due to super saturation.

3. Emulsions with varying tween (sample 12 to 16)   affect the stability of the emulsion, they only impacted the texture i.e. the emulsions with least tween was less foamy as compared to the one with maximum tween. Sample 15 with adequate amount of tween i.e. 15ml showed most acceptable results as the emulsion was ot highly foamy with least settlement.

4. Emulsions with varying Cobalt ferrite nano particles showed change in color.

On the basis of the above mentioned observations two samples were selected with best stability, i.e. sample 8 and 15. In order to confirm the stability of the emulsions, 2 emulsions of each sample 8 and 15 were formulated on the basis of the second parameter that is varying sonication cycles.

Following are the specifications for the adjustment of the second parameter of sonication cycles.

Codes	Solvent (ml)	Polymer (mg)	Surfactant (ml)	Nanoparticles (mg)	Drug (mg)	Sonication Rate
	Ethanol	Eudagrit 100	Tween 80	$Co_2Fe_4O_6$	MTX	Amplitude 60% at 20 kHz
E 8(A)	6	150	2	3	10	2 minutes, 1 pulse off 4 pulses on Cycles 20/min
E 8(B)	6	150	2	3	10	2 minutes, 1 pulse off 4 pulses on Cycles 12/min
E 15(A)	6	150	2.5	3	10	2 minutes, 1 pulse off 2 pulses on Cycles 20/min
E 15(B)	6	150	2.5	3	10	2 minutes, 1 pulse off 4 pulses on Cycles 12/min

Table 3-3-3 Conditions for selected emulsions

Sample with labeling A and B were formulated by varying sonication speed. In Sample (A) sonication was done at 2 minutes, 1 pulse off 2 pulses on Cycles 20/min, whereas sample (B) were sonicated at longer pulses in probe sonicator i.e. 2 minutes, 1 pulse off 4 pulses on Cycles 12 /mi, both at amplitude of 60% at 20 kHz.

Following are the observations:

1. Emulsion Sample 8(A) with low sonication rate, showed the stable emulsion with slightly high settlement of the particles

2. Emulsion Sample 15(A) with low sonication rate showed the most stable emulsion with least settlement of the particles and homogeneity due to more cycles.

3. Emulsion Sample 8(B) with high sonication rate showed stable emulsion with slightly high settlement of the particles.

4. Emulsion Sample 15(B) with high sonication rate showed the most stable emulsion with slightly high settlement of the particles due to fewer cycles.

Sample 15(A) was opted due to best outcomes in terms of stability at ambient conditions. 2 samples of sample 15 i.e. with treated nanoparticles ad untreated nanoparticles were characterized by varying characterization techniques.
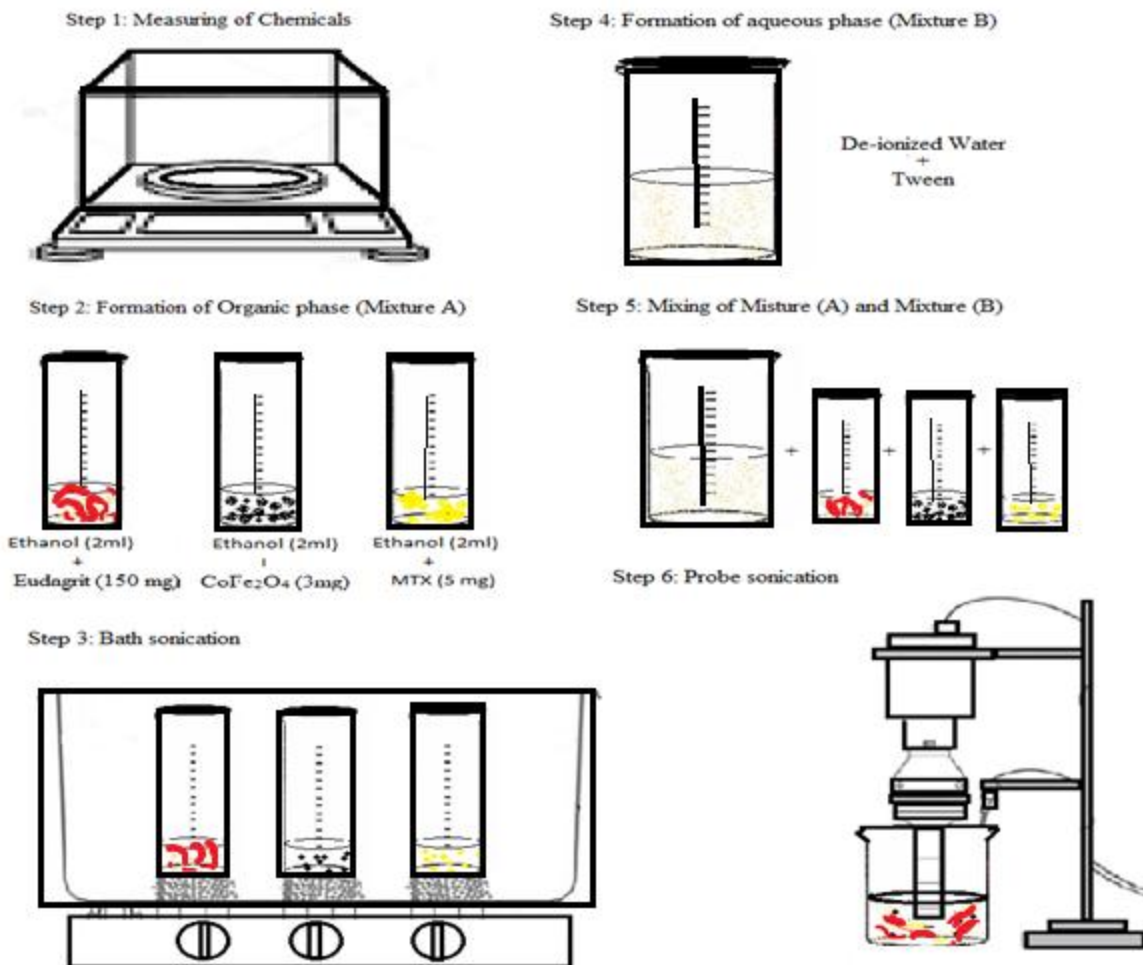
Fig 3.8 Detailed schematic of the emulsion formation

3.6 Physical Appearance:

The physical appearance of prepared emulsion was translucent greenish in color. The nanoemuslion was stable at room temperature an in refrigerator up to 1year. Sonicator or homogenizer both can be used for the nanoemulsion, but the stability achieved from sonicator lasts long. Small amount of precipitates of cobalt ferrite particles were observed that easily redispose on manual mechanical shaking for few seconds.

Physical appearance	Translucent greenish-yellow nanoemulsion (un treated)	Translucent brownish-yellow nanoemulsion (treated)
Suspendibility	No aggregates	No aggregates
Signs of Instability	No Caking, No creaming or separation of phases	No Caking, No creaming or separation of phases
pH	7.01	6.80

Table 3-3-4 Physical and chemical Properties

The nanoemuslion showed some large circle's with entrapped particles at micro scale.
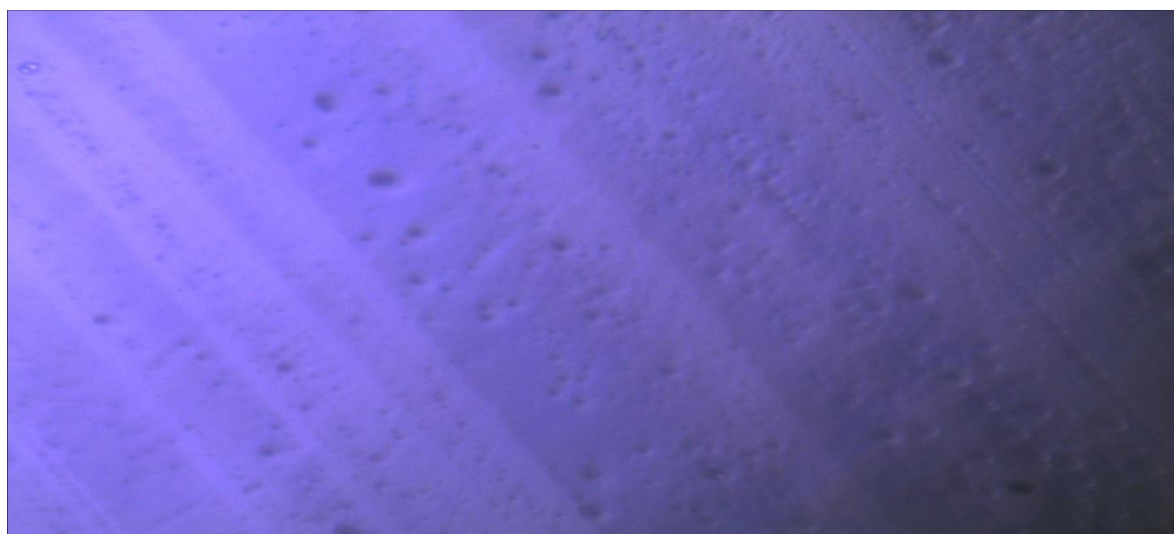
Fig 3.9 Optical Microscopy of E15 at 50 x
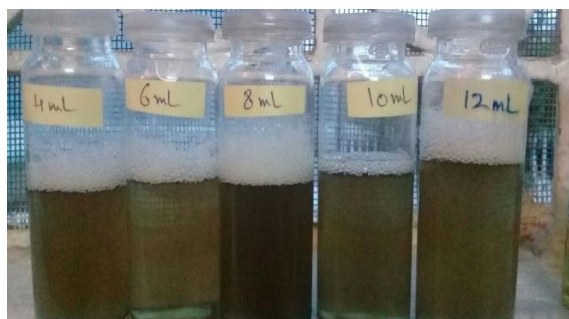
(a) Emulsions with varying ethanol

(b) Emulsions with varying polymer

(c) Emulsions with varying tween

(d) Emulsions with varying particles $Co_2Fe_4O_6$

Fig 3.10 Images of Emulsions

Limitations:

Following are the limitations:

➢ Sonication of the magnetic particles should be done for minimum of 30 minutes at least, because particles agglomerate in emulsion.

➢ Grade of eudagrit in crystalline form should be used as powdered eudagrit forms thread like structure when poured drop wise into the mixture.

➢ Methotrexate should only be stirred with the magnetic stirrer without heating, because it is temperature sensitive.

➢ Ethanol must be evaporated in Rota evaporator not by overnight stirring on Magnetic plate as magnetic particles will stick to the magnetic stirrer and will affect the stability of the emulsion.

Centrifugation and Lyophilization of nanoemulsion:

Eudagrit coated methotrexate cobalt ferrite loaded nanoemulsion was centrifuged at 13,500 RPM for 1 hour. Procedure was repeated twice for proper washing and removal of entrapped drug and pellets were collected. Then 5ml of ethanol was mixed with the pellet and mixed thoroughly. The purified nanoparticles were incubated at -80 oC for 24 hours. Afterwards the frozen samples were lyophilized to get solid nanoparticles. Freeze drying removes water from freeze dried samples by sublimation process. Firstly turned on the lyophilizer and adjust temperature to -76 ^{o}C and pressure to 0.014 mbar. Press warm-up vacuum phase for vacuum creation. Once vacuum is generated than main drying starts and continues for 6 hours. Then continue with the final drying phase that lasts for 6 hours and solid nanoparticles were obtained. Particles showed greasy texture due to presence of surfactant due to which procedure was repeated twice so that completely dried nanoparticles could be obtained. Following figure shows setup for oil in water simple emulsion technique.

Ethanol (2ml) + Eudagrit   Ethanol (2ml) + CoFe$_2$O$_4$ Ethanol (2ml) + MTX ⏐   De-ionized Water + Tween   Probe sonication   O/W   Coated MNP

Organic phase (Mixture A)   Aqueous phase (Mixture B)   Centrifugation and Lyophilization
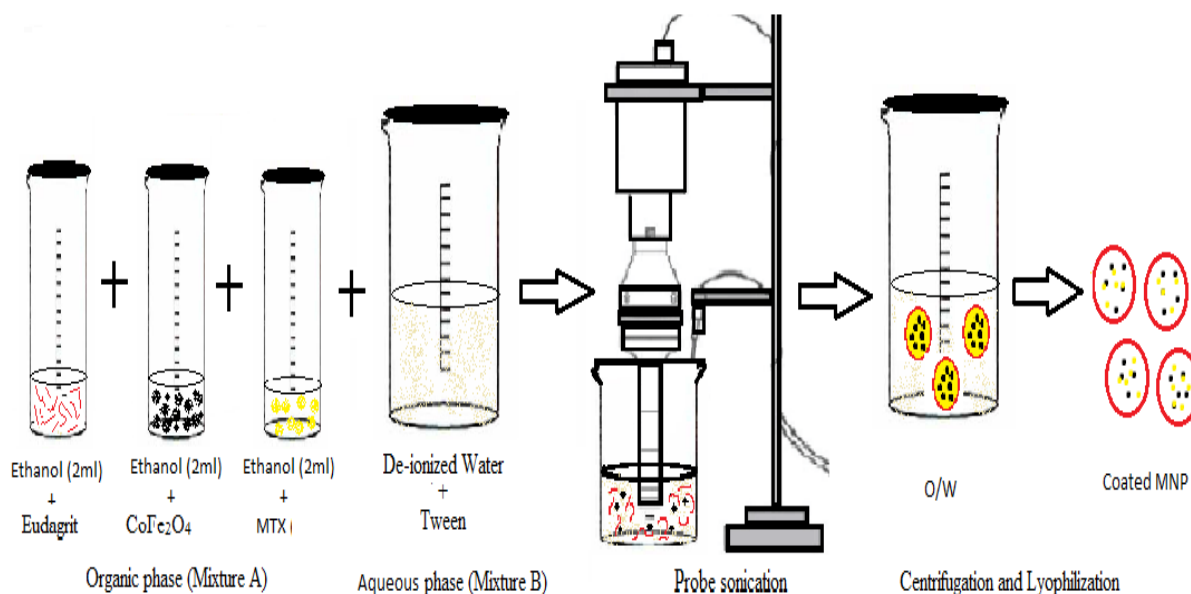
Fig 3.11 O/W emulsion technique

4 Chapter 4: Solution Validation, Analysis of the Data, Results, and Discussion

After the stable emulsion was selected characterization was performed. Study of Magnetic Properties of iron Cobalt Nano particles using Vibrating sample Magnetometer (VSM). The chemical composition of magnetic nano particles, and solid and liquid content of emulsion was evaluated by X-ray Diffractometer (XRD). Similarly charges, polydispersity Index (PDI) and size of particles in emulsion were found by Zeta potential. Microscopy at micro and nano level was performed by Optical microscope and Scanning electron microscope (SEM). Encapsulation of the drug was evaluated by UV-Vis, likewise encapsulation of solid content of magnetic nanoparticles in emulsion was done by Thermo-gravimetric Analysis (TGA/DSC).

Following are the characterization techniques that are conducted:

4.1 Validation of magnetic properties of nanoparticles:

Validation of the magnetic properties of the nanoparticles was performed by VSM at Punjab University, Center of Excellence of solid state physics.

4.1.1 Vibrating Sample Magnetometer (VSM)

It is a sensitive and versatile instrument for study of magnetic moments in different magnetic materials as a function of magnetic field and temperature. Its use to measure magnetization is based on the Faraday's laws of electromagnetic induction. The vibrating-sample magnetometer has been in use for routine magnetic measurements as a function of temperature and field of ferromagnetic, ferrimagnetic, antiferromagnetic, paramagnetic, and diamagnetic materials [60].

Magnetism is a sub-atomic phenomenon and is mainly caused due to the polarization of electric clouds, or magnetic dipoles of certain materials with unpaired electrons. Due to this imbalance, the atom gains a net angular momentum, and a magnetic field perpendicular to the rotation of spin of the excess charge is caused. This spin-spin interaction classifies materials into different magnetic classes. In most materials, the spin moments are small and aligned randomly, causing to paramagnetic behavior. In some materials, specifically transition metals such as nickel, cobalt, and iron, the spin moments are large, and align in parallel or ferromagnetically [61]. This causes a net spontaneous magnetic moment in the material.

The magnetic target drug delivery system has various applications in the field of cancer treatment. And its value depends on whether the system possesses super paramagnetic, biocompatibility, effectiveness of drugs and otherwise [62].

The sample to be studied is kept in a constant magnetic field. If the sample is magnetic, this constant magnetic field will magnetize the sample by aligning the magnetic domains, or the individual magnetic spins, with the field. The stronger the constant field, the larger the magnetization will be. The magnetic dipole moment of the sample will create a magnetic field around the sample, sometimes called the magnetic stray field. As the sample is moved up and down this magnetic stray field changes as a function of time and can be sensed by a set of pickup coils. Using controlling and monitoring software, the system can tell us how much the sample is magnetized and how its magnetization depends on the strength of the constant magnetic field. The output is a hysteresis curve, which shows the relationship between the induced magnetic flux density and the magnetizing force and gives important information about the magnetic saturation, the remenence, the coercivity and the level of residual magnetism left in the material.

Result and discussions:

 Initial hysteresis curve is paramagnetic till the saturation magnetization. Afterwards the curve is ferromagnetic. The behavior of the sample is highly dependent on acid treatment, size and the aggregation formed in it. Initial behavior of the sample is paramagnetic, where the magnetic moments align in the direction of applied field to build up a net magnetization, reaching saturation magnetization with the increasing field. When the field is reversed the magnetic moments reorient in the direction of this opposite field. It is to be noted that for zero field there is non-zero magnetization called remenence or retentivity which is 1.343 emu. The magnetization become zero after applying further field in opposite direction and the value of field at that point where magnetization reaches zero is called coercivity. Basically, coercivity is the resistance of a magnetic material to changes in magnetization, equivalent to the field intensity which is 1549.6 G. It is necessary to demagnetize the fully magnetized material. This behavior is ferromagnetic where the remenence and coercivity is non-zero. Coercivity, magnetization and retentivity decreased almost to half due acid treatment. But particles showed magnetic properties due to which it can be used for magnetic emulsions. The initial paramagnetic and then ferromagnetic

response indicates that the sample particles have size greater than the size required for supper paramagnetic behavior, the magnetic behavior of magnetite nanoparticles changes accordingly with their size. Below are the results that are obtained by VSM:

Coercivity (Hci)	1549.6 G
Magnetization (MS)	2.6056 emu
Retentivity (Mr)	1.3404 emu

Table 4-4-1 Magnetic Properties

Following is the hysteresis curve:
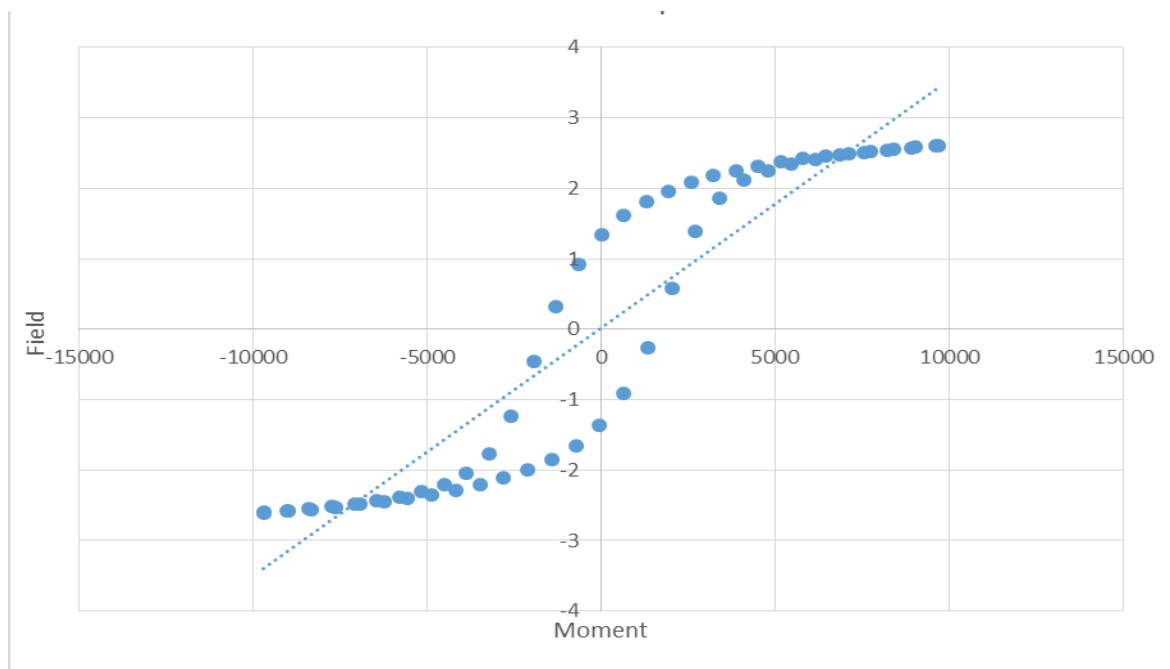
Fig 4.12 Hysteresis loop iron cobalt nanoparticles.

4.2   Validation of chemical composition of nanoparticles

Validation and Examination of the crystallographic phases of the sample was performed using GNR explorer diffractometer in IST, Islamabad.

4.2.1   XRD (composition)

X-ray diffraction is a technique in which a beam of x-ray is diffracted on to the material in order to determine its crystallographic properties such as atomic and molecular structure. X-ray are diffracted at an particular angle by the crystalline structure of the nanoparticle, by calculated the

intensities of the diffracted beams density of the electronic clouds are evaluated, which help in the determination of the mean position of the atoms in the crystal structure. XRD was carried out in the GNR Explorer, make Italy in IST.

X-ray analysis of the sample is performed in three steps:

1. Firstly adequate amount of powder nanoparticles that are under study were mounted for measurements, so that it could be held in the x-ray beam and rotated.
2. Secondly nanoparticles were placed in the monochromatic x-ray beam producing regular pattern of reflection, sample was gradually rotated at 2θ between 30° to 90°, and new set of reflections was obtained at every rotation. Intensity of every spot was recorded; multiple data sets were collected covering more than half of full rotation of the sample.
3. Thirdly all data is combined computationally. Experimental results were compared with the bibliographic data from Natta, Passerini. Gazz. Chim. Ital. 59,286 (1929).

4.2.2   Data analysis: Cobalt ferrite nano particles:

Reflection from the each crystallographic plane of the nanoparticles are indexed in data processing, each reflection corresponds to the density of atoms present in the crystallographic plane, which are plotted in the graph. One of the major issue in the determination of the sample is the disorder crystallographic structure, it occurs due to co-existence of 2 or more elements or conformations. Flawed interpretation could result from the failure to recognize the defect. Results from the testing were later deposited in the crystallographic database, i.e. Natta, Passerini., Gazz. Chim. Ital. 59,286 (1929). Comparison was run by the software and most accurate match was found, corresponding to the properties of the nanoparticles. Following are the diffraction data:

Diffraction data

d[Å]	Int.	hkl	Remark
2.960000	30	220	hkl generated by input software
2.520000	100	311	hkl generated by input software
2.090000	40	400	hkl generated by input software
1.710000	20	422	hkl generated by input software
1.610000	60	511	hkl generated by input software

1.480000	80	440	hkl generated by input software
1.410000	8	531	hkl generated by input software
1.320000	10	620	hkl generated by input software
1.280000	30	-	
1.120000	20	-	
1.090000	60	731	hkl generated by input software
1.050000	30	-	

Table 4-4-2 Diffraction Data

Graph of diffraction pattern is as follows:
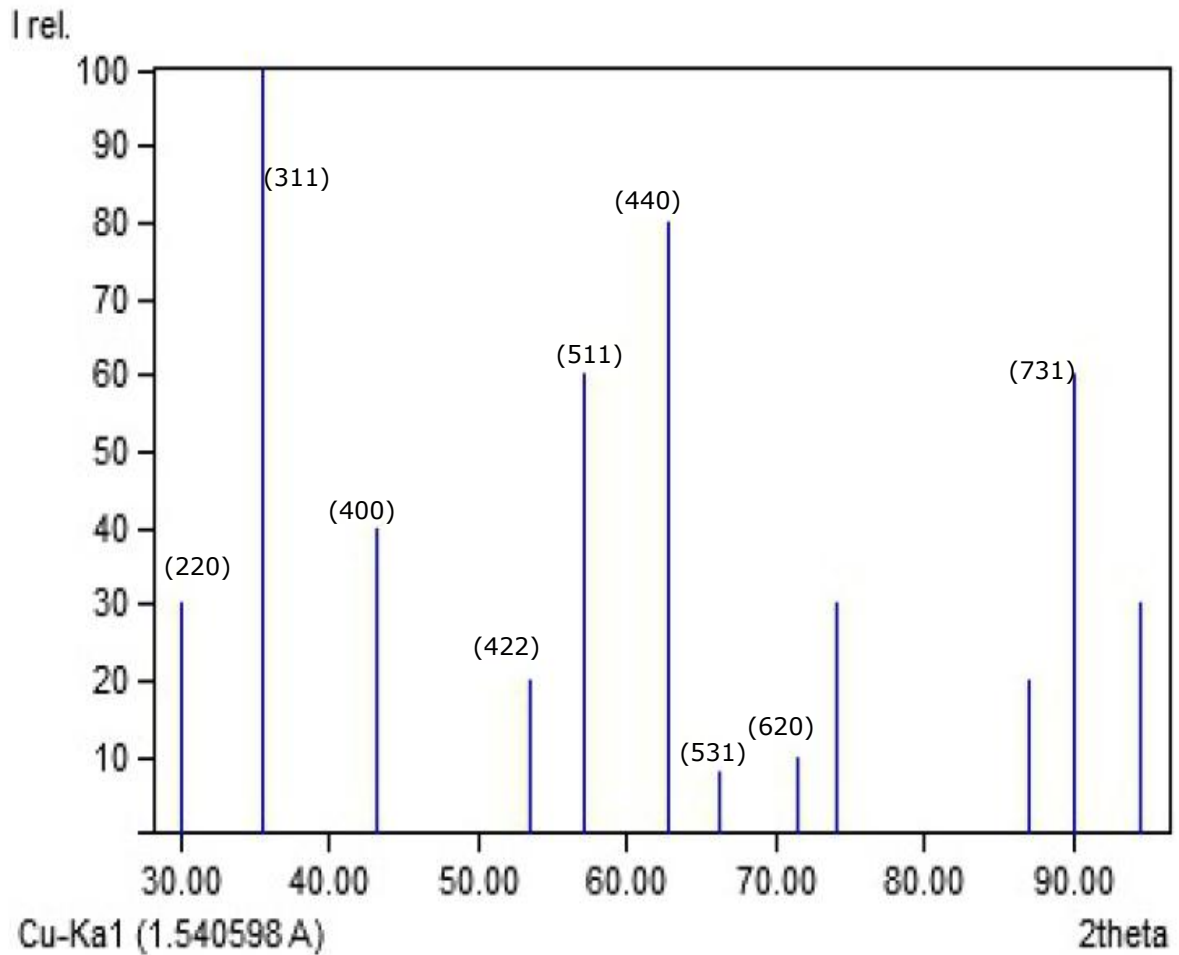
Fig 4.13 Diffraction pattern peaks

Analysis of the diffraction graphics was performed by comparative peak position of the XRD spectra of samples with the standard spinel ferrite compounds using x-ray diffract meter. X-ray crystallographic revealed that the arrangements of the atoms in the crystallite of 2θ values between 30° to 90° to find there different properties. In spinel ferrites atomic structures each cobalt ion occupies one tetrahedral site and each ferrous metal ion occupies one octahedral site. Totally in a unit cell, there will be 8 tetrahedral (8 A) sites and 16 octahedral (16B) sites. Hence, the sites A and B combined to form a regular spinel ferrite.

Given below are the results and classification:

Name	Cobalt Iron Oxide	
Formula	$CoFe_2O_4$	
Pearson symbol	cF56	
Crystallographic data (crystal structure)	Space group	Fd-3m(227)
	Crystal system	Cubic
	Cell parameters	a= 8.360000Å
	Cell volume	584.280029
	Z	8
Physical properties	Measured density	5.300000 g/cm^3
	Calculated density	5.334000 g/cm3
	Color	Black

Table 4-4-3 Phases and Classification

4.3 Magnetic responsive polymer colloids:

The main purpose of the x-ray is to find the density of electrons throughout the crystal plane, which corresponds to the data collected from the X-ray scattering. Intensities of the reflection give magnitude but not the phases. Wavelengths are modulated past a certain absorption edge, or a high density metal such mercury is added in order to get full set of reflection with identified shift to scatterings. Combining magnitudes and phases are incorporated it into Fourier transformation to find density. Following are the X-ray graph of magnetically responsive polymer colloids.
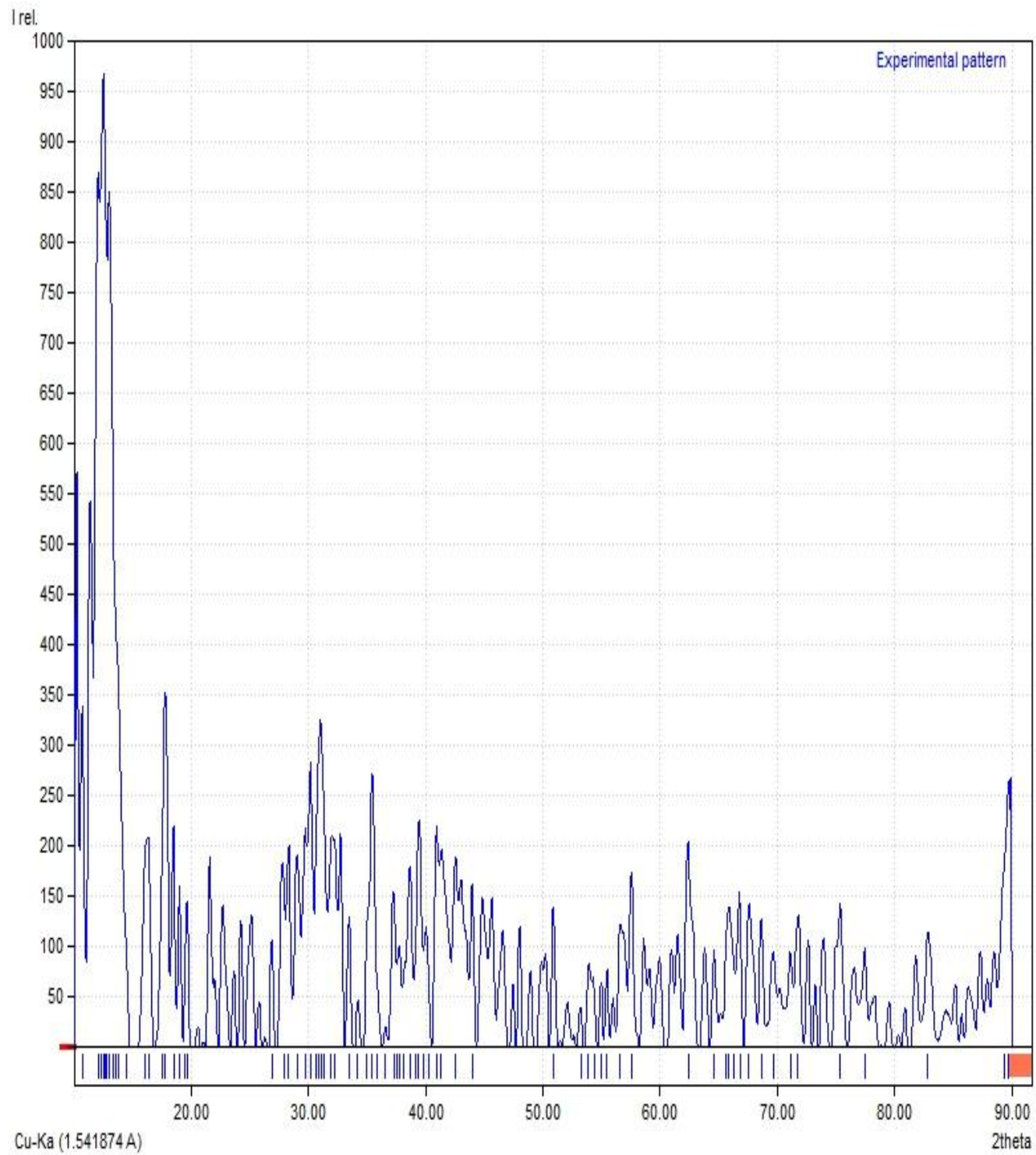
Fig4.14 XRD graph Magnetic Based theranostic nanoparticles

37

Identification of characteristics peaks of Methotraxte:

Peaks are dependent on the lattice energy, for methoteraxate characteristic peaks were obtained. Value of 2 theta for methoteraxate varied from 10.35 to 25.87. Less order phase and weak crystalline structure resulted into small range of peaks.
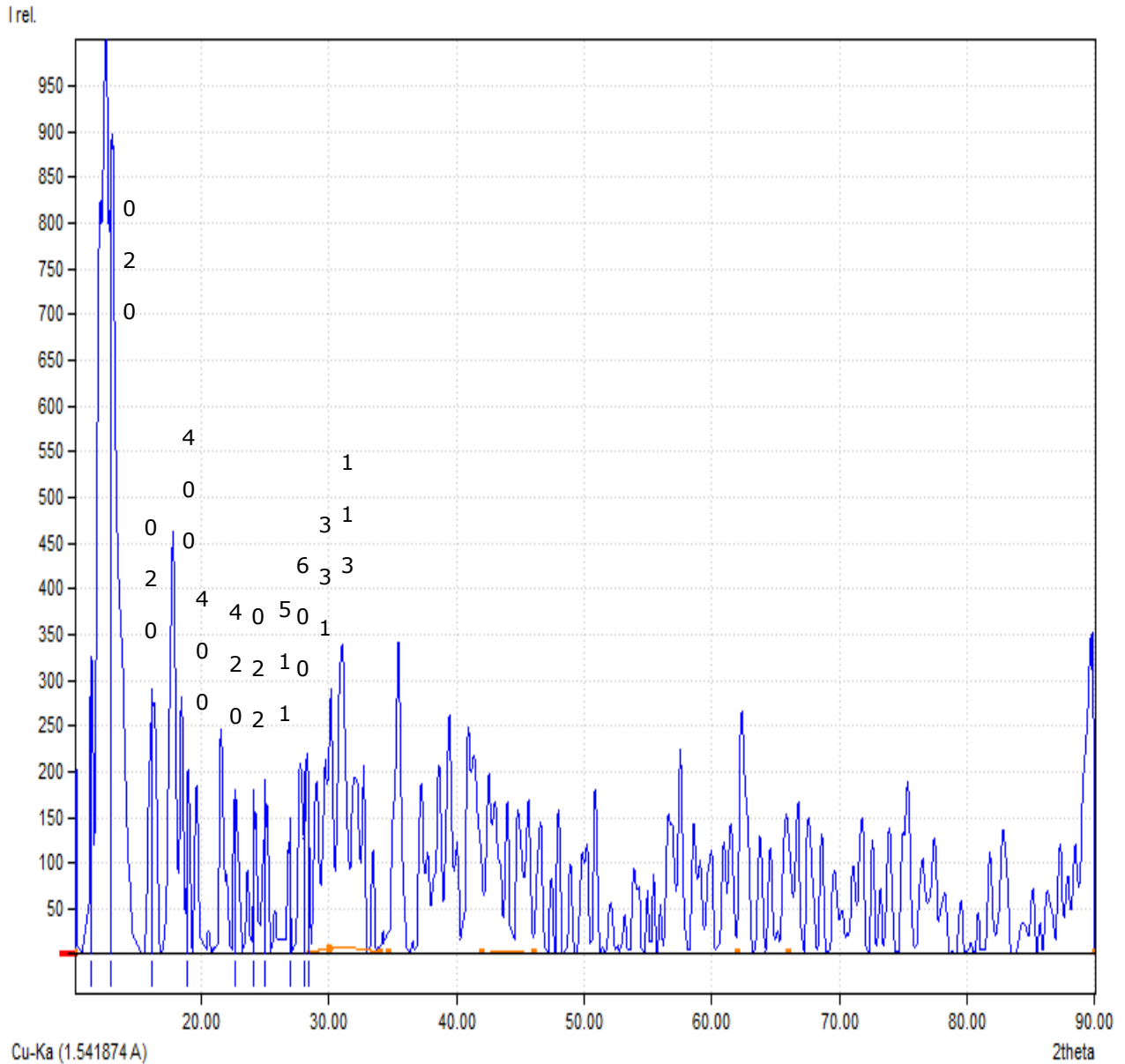
Fig.4.15 Identification of characteristics peaks of Methotraxte

Identification of characteristics peaks of Eudagrit E 100:

Eudagrit showed maximum intensity peaks which is due to high crysttaline structure and presence in large amount. Value of 2 theta varied from 12.08^o to 82.77^o. Large variation in range of 2 theta indicates higher crystalline structure.
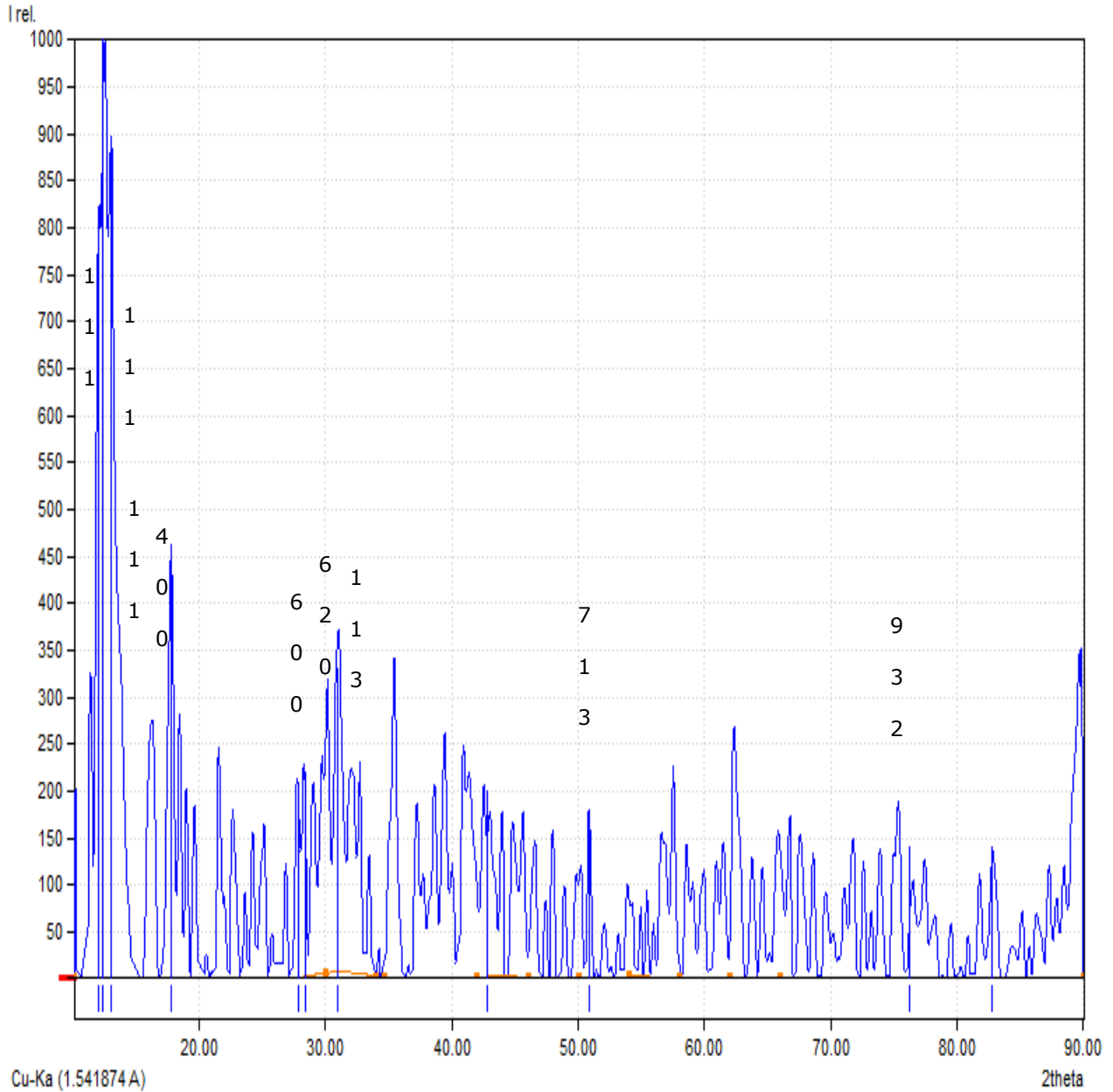
Fig 4.16 Identification of characteristics peaks of Eudagrit E 100

Identification of characteristics peaks of iron cobalt oxide:

XRD pattern peaks were identified from comparative peak analysis fom above results, 2 theta values varied from 30° to 90°. Large order phase and strong crystalline structure resulted into long range of peaks.
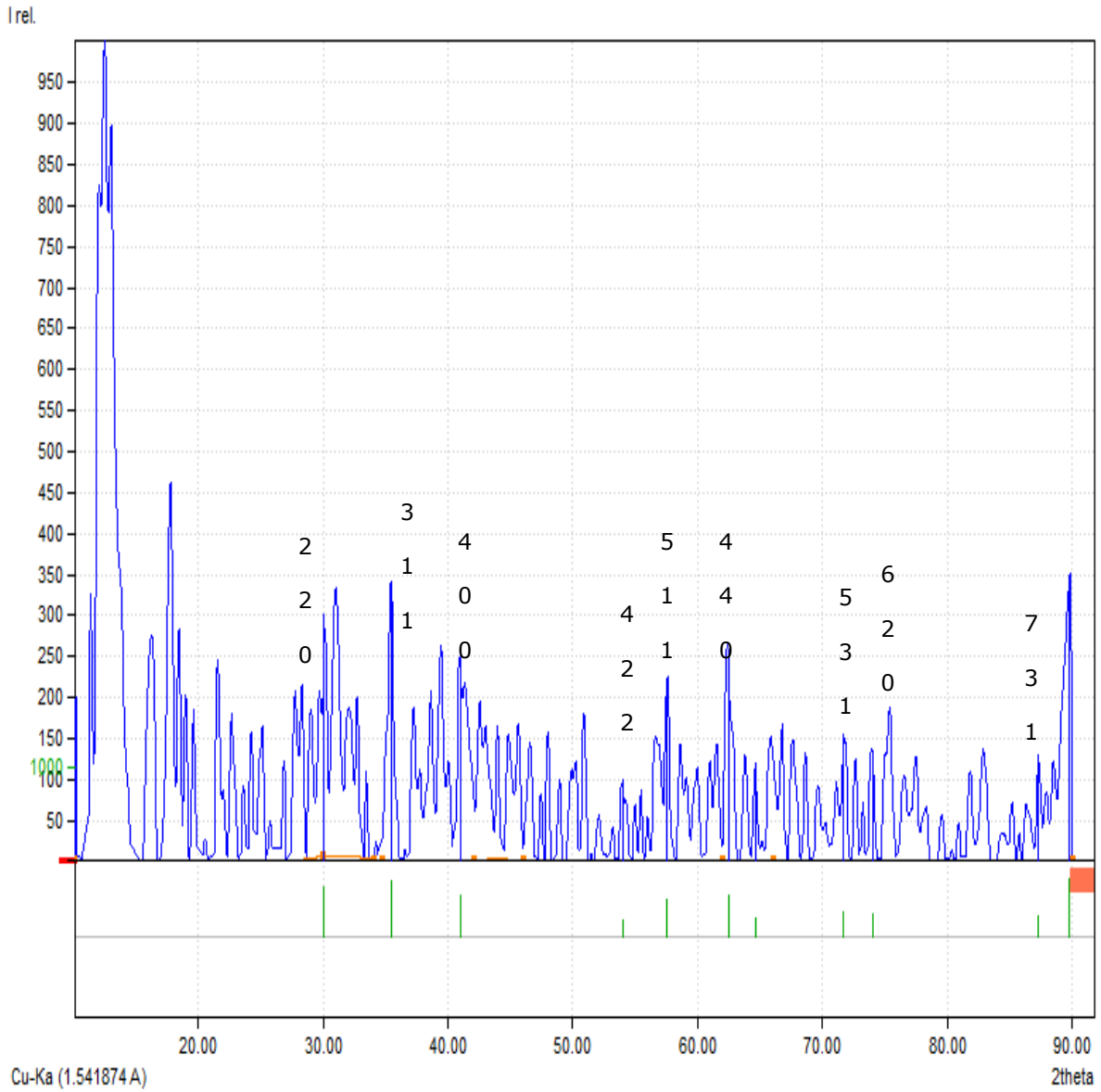
Fig 4.17 Identification of characteristics peaks of iron cobalt oxide

4.4 Validation of size and morphology of nanoparticles

SEM analysis was performed at IST, Pakistan to determine surface morphology and particle size.

4.5 Scanning Electron Microscope (SEM)

The scanning electron microscope (SEM) produces images by scanning the sample with a high-energy beam of electrons. As the electrons interact with the sample signals are produced. These signals are collected by one or more detectors to form images which are then displayed on the computer screen. When the electron beam hits the surface of the sample, it penetrates the sample to a depth of a few microns, depending on the accelerating voltage and the density of the sample. Many signals, like secondary electrons and X-rays, are produced as a result of this interaction inside the sample.

Sample Collection and Preparation

Minimal preparation includes acquisition of a sample that will fit into the SEM chamber and some accommodation to prevent charge build-up on electrically insulating samples. Most electrically insulating samples are coated with a thin layer of conducting material, commonly carbon, gold, or some other metal or alloy. The choice of material for conductive coatings depends on the data to be acquired: carbon is most desirable if elemental analysis is a priority, while metal coatings are most effective for high resolution electron imaging applications. Alternatively, an electrically insulating sample can be examined without a conductive coating in an instrument capable of "low vacuum" operation. [63].

Sample for SEM was prepared by sonication of 1 mg of nanoparticles in 3 ml of ethanol for 30 minutes. Later drop of mixture was placed on clean glass slab, ethanol was evaporated. Later gold sputtering was performed in order to get high resolution results.

Surface morphology of iron-cobalt nanoparticles: Magnetic nanoparticles were observed and examined. SEM images showed spherical shaped nanoparticles and particle size with range of 23-25 nm.
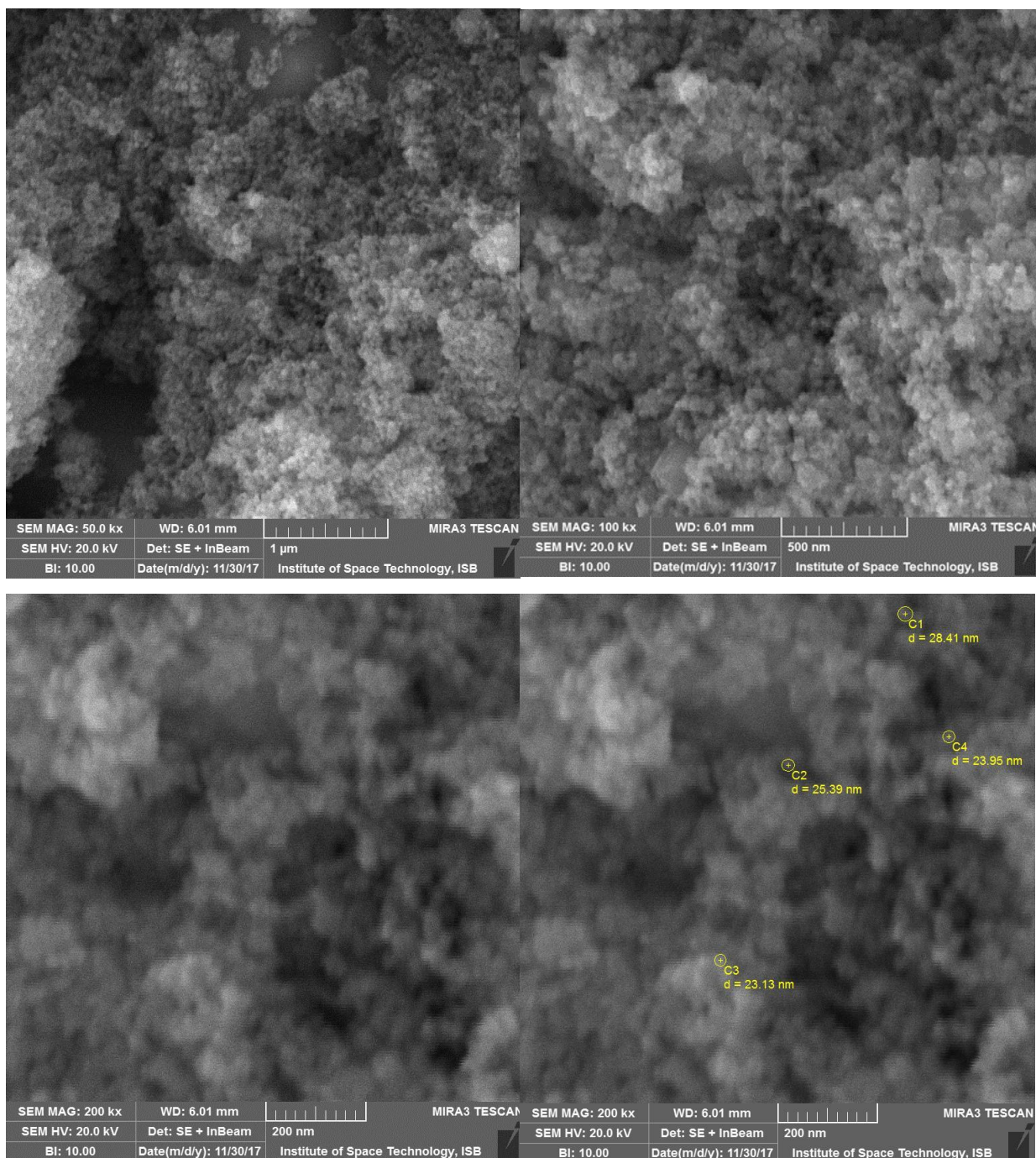
Fig 4.18 SEM images of magnetic particles cobalt iron oxide

Surface morphology of magnetically responsive polymer colloids:

Methotrexate loaded heat sensitive coated Eudagrit S100 showed spherical shaped nanoparticles. Particle size is of great importance as the particles that are <10 nm are excreted whereas elements that are >200 nm get stuck as a result of the mechanical separation. Particles size within

range of 10-100 nm is optimal for this type of applications. Sample was prepared by diluting 1ml of emulsion in 5ml of distill ad allowing the drop on glass chip to air cool, as heating on hot plate to dry the sample could not be done because of polymer. After 2 hours of drying sample was analyzed. Particle size particle size with range 47-53 nm was obtained which depicts coating of polymer over magnetic particles with encapsulated drug.
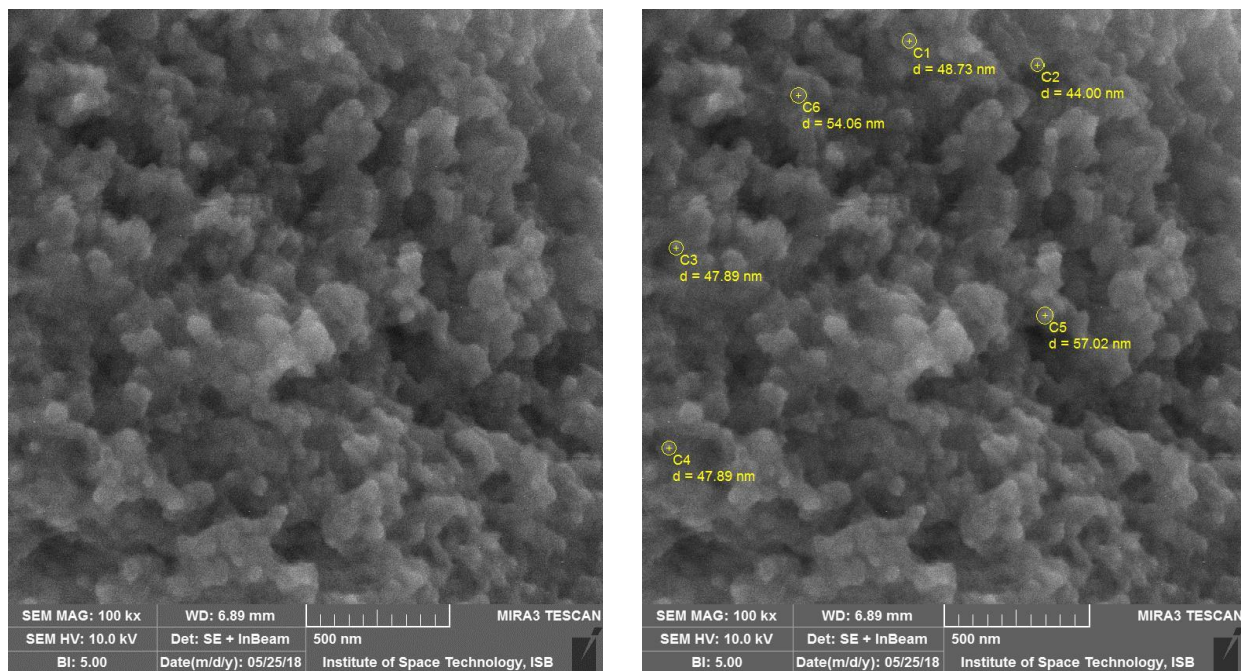
Fig 4.19 SEM images of MBTN synthesized with iron cobalt nanopaticles

4.6   Encapsulation of solid content:

Analysis of the solid content in emulsion was evaluated by DTG-60/60H -Shimadzu at U.S.-Pakistan Center for Advanced Studies in Energy (USPCAS-E), NUST.

Differential Thermogravimetiric Analysis (DTA)

Thermogravimetiric analysis is a technique in which sample is subjected to heating and changes in the mass of the sample is evaluated against temperature. It is not necessary that all the events occurring during thermal heating bring about changes in the mass. Samples were heated in aluminum pan from 0 ^{o}C to 600 ^{o}C at rate of 10 ^{o}C/min in an inert atmosphere.
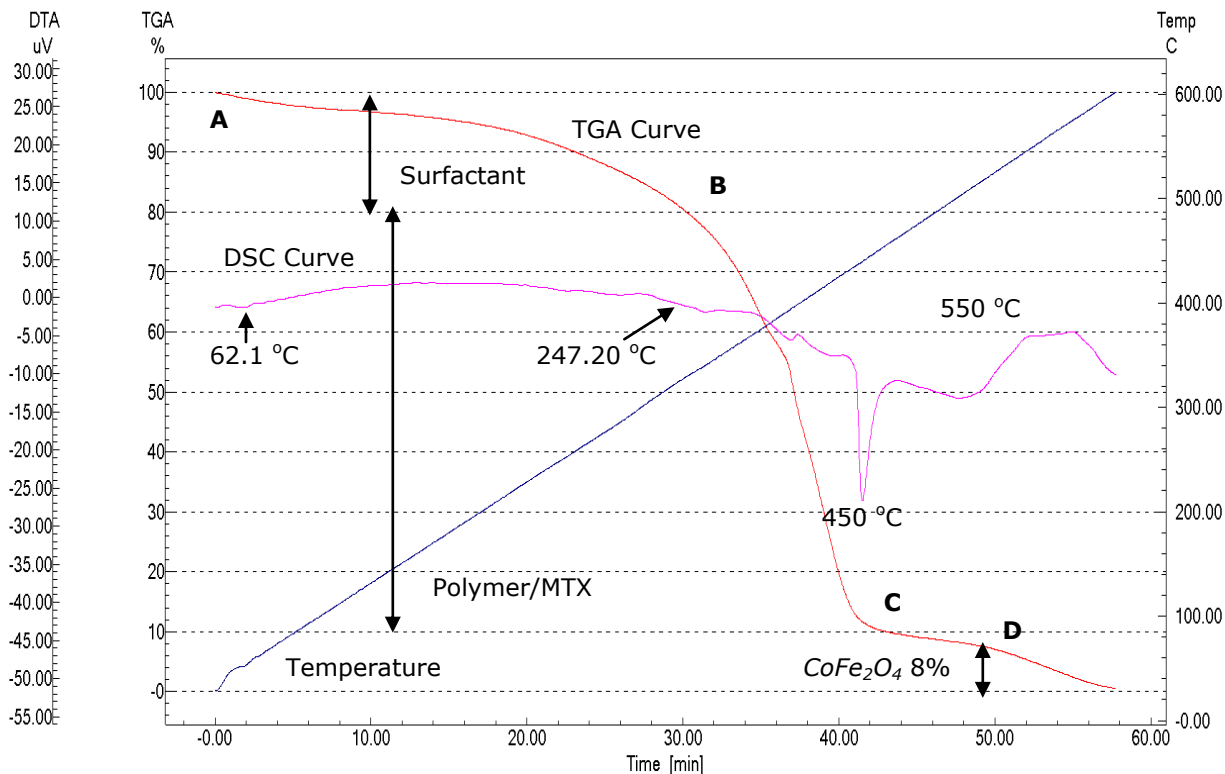
Fig 4.20 TGA/DSC thermograms of lypholized samples

Results and Discussion:

Thermograms of emulsion composed of treated nanoparticles and untreated nanoparticles were compared. All the volatile product, polymers and nanoparticles in the emulsion were evaluated by testing and should exothermic reactions. Thermal events like absorption desorption and decomposition brought changes in the mass of the sample. Results of DTA demonstrates three unique thermograms, blue thermogram indicate linear change in temperature with time, Red thermogram shows results of TGA, that is loss in mass due to decomposition, desorption or absorption, pink thermogram shows results of DSC.

Peaks pointing downward indicate endothermic reactions occurring during heating, which results in the downward shift of TGA curve due to loss of mass as result of decomposition. Peaks pointing upwards indicate exothermic reaction which caused shift of the TGA curve.

Analysis of DSC curve: Thermal curve showed characteristic peak at 62.1 ^{o}C compared to the melting point of Eudagrit e 100. At 247.20 ^{o}C decomposition of methotrexate started followed by endothermic depression, small depression in the endo-curve is due to transition from solid to solid state. Baseline of TGA curve slightly lowered after melting at 450 ^{o}C, which indicates that

44

absorption of heat is less for liquid as compared to the solid. Melting at 450 $^\circ$C indicates complete decomposition of the organic phase in sample. At 550 $^\circ$C rise in thermal curve is observed which is due to the presence of crystalline inorganic iron cobalt nanoparticles.

Analysis of TGA curve: At 100% percent at point A temperature is 25 $^\circ$C as the temperature is increased from point A to B approximately 20% of the total volatile mass mainly surfactant has evaporated. From point B to C there is very steep curve with 70% loss in mass due to evaporation of polymer which constitutes largest mass in the sample. Nanoparticles emulsion total mass of 8-10% is left at the end of the processes which indicates un-decomposed iron cobalt nanoparticles which are left due to their high melting temperature if 1567 $^\circ$C.

4.7   Validation of charge on nanoparticles

Zeta potential for methotrexate loaded pH sensitive nanoparticles was determined by Malvern Zeta sizer at Quaid-e-Azam University, Islamabad.

4.7.1   Zeta potential for charge

It is the difference between the stationary layer and the moving layer in the dispersion. It is electrostatic difference between the negative and positive particles present in the dispersion, and one of the factors that determines the stability. It is main indicator for the stability of the colloidal dispersion. When particles are small they have higher values of zeta potential due to which, repulsive forces are higher and colloidal solution doesn't aggregate. Whereas when the particles are larger they have low zeta potential due to attractive forces dominate and particles in the colloidal solution coagulate, hence suspension collapses. Zeta potential is basically the difference the electrostatic repulsive forces between the particles that are preset in the colloidal solution It was performed in triplicate. It is mainly used for the quantification of the net charge, because zeta potential is actually the sum of the total charge contained in the colloidal suspension

In colloidal suspension potential is applied across the suspension due to which particles migrate to opposite charged electrodes. Negative particles will go towards the positive electrode with the velocity relative to the magnitude of the potential and positive change will do vice versa. The velocity with which the particles move towards the electrode is measured by the Doppler laser. By putting viscosity and electric permittivity in the Smoluchowski theories, zeta potential is evaluated.

4.7.2 Particle Size and Zeta Potential Analysis Protocol

The particle size, distribution and zeta potential of the samples were determined using dynamic light scattering utilizing the Zetasizer Nano ZS 90 (Malvern Instruments; Worcestershire, UK), equipped with software (version 6.34) and a He-Ne laser at a wavelength of 635 nm and static scattering angle of 90 degree. Briefly 10 µl of the sample was mixed with 1 ml of deionized water and vortexed for 2 minutes followed by analysis with zetasizer. Each result displayed was measured in triplicate (Din et al 2015a,b; Din et al 2017a,b). [66] [67][68][69]

Results and Discussions:

Positive values of zeta potential indicates the positive charge around the nano particles, it is desirable as it stabilizes the formulation and prevents aggregation. Values of zeta potential indicate incipient stability. When it approaches zero aggregates of the nanoparticles are formed. Particle size average is 188.3 nm, which indicates that particles of lesser size are also present. PDI value is low which is indication of average charge distribution is uniform throughout the sample. Following are the zeta potential results of emulsion:
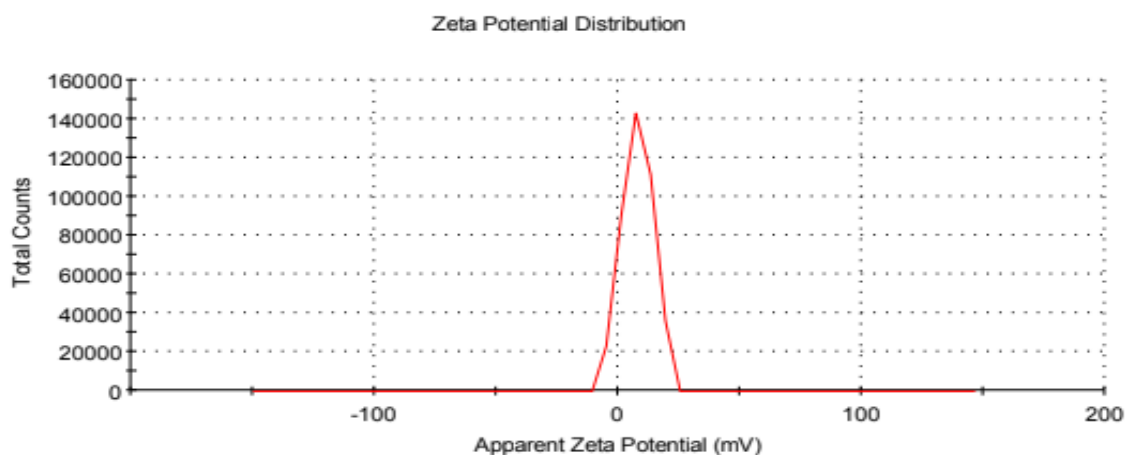

Fig 4.21 Zeta potential charge distribution

Zeta potential (mV)	8.96 ± 6.16
Conductivity (ms/cm)	0.82
PDI (0-1)	0.097

Table 4-4-4 Zeta potential

4.8   Characterization and evaluation of Methotrexate in pH sensitive nanoparticles:

Characterization and evaluation of methotrexate loaded pH sensitive nanoparticles was done by evaluating percent yield and encapsulation efficiency of iron cobalt nanoparticles in Magnetic based theranostic nanoparticles.

4.8.1   Percentage yield (%)

Percentage yield was found by calculating the total weight of polymer, drug and excipient to find theoretical amount of nanoparticles. Then weigh solid freeze and excipient to find theoretical amount of nanoparticles. Then weigh solid freeze dried drug loaded nanoparticles, percent yield is calculated by following formula:

$$\text{Percentage yield (\%)} = \frac{weight\ of\ the\ magnetic\ based\ theranostic\ nanoparticles}{weight\ of\ the\ (polymer+drug+iron\ cobalt\ nanoparticles)} \times 100$$

$$\text{Percent yield (\%)} = 42.40\ \%$$

4.8.2   Encapsulation efficiency:

Calculation of encapsulation efficiency involved collection of supernatant after three times centrifugation of the nano-formulation. 1ml of this supernatant was analyzed to know "free drug" content in it by UV-Vis Spectrophotometer. Drug concentration was found from absorbance values at wavelength of 302 nm from given formula and encapsulation efficiency was calculated.

Ultraviolet-Visible spectroscopy:

UV visible spectroscopy was performed on the samples in order to find out the methotrexate encapsulation in the magnetic emulsion. For his purpose 2 emulsions were, one was blank (emulsion with no drug contained in it and other carried the drug so that comparison could be made. Blank was labelled has reference cell and other contained the sample.

4.8.2.1   Formation of Calibration Curve of Methotrexate in Phosphate Buffer (pH 7.4)

Calibration curves were made in order to find out the drug concentration in the buffer, for this 10 mg of drug was dissolved in phosphate buffer by sonicating it for 10 minutes in sonicator and total volume was made up to 100ml with phosphate buffer, after that 6 serial dilutions were prepared, and were analyzed at wavelength of 302 nm by UV- Vis spectrophotometer. MS excel was used to plot curve that was further used for measurement of in vitro drug release and drug content.

Sample No.	Conc.	Abs 1	Abs 2	Mean
1	3.12µg/ml	0.736	0.757	0.7465
2	1.562µg/ml	0.357	0.397	0.377
3	0.781µg/ml	0.173	0.212	0.1925
4	0.390µg/ml	0.083	0.119	0.101
5	0.195µg/ml	0.1	0.134	0.117
6	0.097µg/ml	0.039	0.032	0.0355

Table 4-4-5 Calibration curve Data

Following is calibration curve of methotrexate at 252nm. Absorbance is taken on y axis and concentration is taken of x axis.

y = 0.236x + 0.0091
R^2 = 0.9997
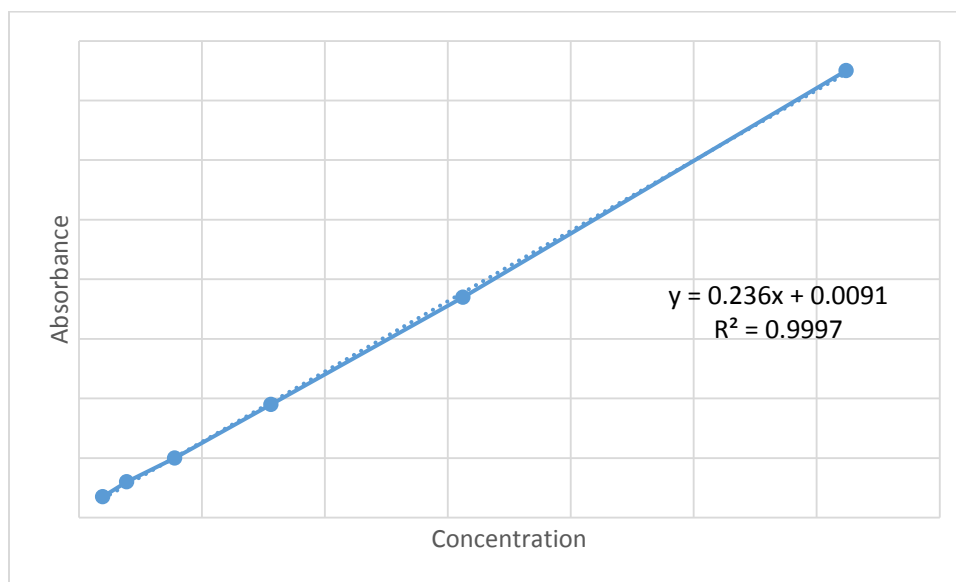
Fig 4.22 Calibration curve of Drug

Results and discussion:

Light intensity passing through each cell was evaluated over entire range of the wavelength, if value of reference cell intensity (I_0) is greater than sample intensity (I) than it means the sample has absorbed some light due to presence of the MTX in the emulsion. Following are the absorbance values for 5 readings:

Sample |code	Absorbance value
1	0.363
2	0.365
3	0.567
4	0.568
5	0.797
Mean	0.532

Table 4-4-6 UV values for drug in supernatant

Drug content was evaluated by using following formula:

y = 0.236x+0.0091

x = (0.532-0.0091)/0.236

Where,

y = Absorbance mean

x = Drug content

Adding in formula gives value of drug in supernatant= 2.21 mg

Following are the graph of readings, five readings were take with time lapse of 1 sec. time is plotted o X-axis and absorbance value is plotted on y-axis, graph pattern shows more linear trend for emulsion that is formed by treated than untreated.

Value of Drug:

$$\text{Encapsulation of Drug (\%)} = \frac{Total\ Drug - Free\ Drug\ in\ supernatent}{Total\ Drug} \times 100$$

$$= 77.9\ \%$$

4.9 In-vitro testing of Methotrexate loaded pH sensitive nanoparticles:

Drug release is a mechanism in which the drug is initially released from polymer shell, then it diffuses through the shell into the release system [70]. Drug release study was carried out in vitro in a stimulated basic pH to find out drug release profile.

4.9.1 In vitro drug release study:

This testing was carried out to ensure drug release at stimulated ph of 7.4 pH. Emulsion will be intravenously administered for this purpose pH was kept near pH of human blood. For this purpose phosphatase buffer of pH 7.4 was prepared.

Preparation of phosphate buffer (pH 7.4)

1. First 0.2 M NaOH was prepared by adding 27.22 g pellets of NaOH in 100 ml distill water.
2. Then, 0.2 M KH_2PO_4 was prepared by adding 8 g of KH_2PO_4 in 1000 ml of distill water.
3. *Buffer solution of pH 7.4*: for preparation of pH 7.4 buffer solution, 50ml of 0.2 M KH_2PO_4 and 39.1 ml of 0.2 M NaOH were mixed along with distill water in order to make total volume of 200ml.

4.9.2 Drug content in final formulation:

With the help of micropipette 5ml of emulsion was encapsulated membrane and was dipped in 50ml buffer solution in conical flask. Conical flask was placed in mechanical shaker for 48 hours for drug release study. Sample of 1ml was taken out from the buffer solution in conical flask at fixed interval. fresh buffer should be added in conical flask equal to the amount taken out so that total volume remains the same. Total nine samples were collected at time terminal of 48 hours all samples were then analyzed at wavelength of 302nm on UV-Vis spectrophotometer using phosphate buffer as reference, For this 0.5 ml of the sample was diluted with 4.5 ml distill water. Following are the readings of UV-Spectrophotometer:

Sample Code	Time t	Reading 1 R_1	Reading 2 R_2	Reading 3 R_3	Reading 4 R_4	Reading 5 R_5	Mean R
A	0.5 hrs	0.127	0.127	0.128	0.128	0.129	0.128
B	1 hrs	0.193	0.198	0.199	0.199	0.201	0.193
C	2 hrs	0.197	0.200	0.203	0.204	0.205	0.202
D	4 hrs	0.209	0.210	0.210	0.211	0.211	0.210
E	8 hrs	0.290	0.291	0.292	0.299	0.301	0.295
F	12 hrs	0.320	0.321	0.322	0.323	0.325	0.322
G	24 hrs	0.350	0.351	0.354	0.355	0.360	0.354
H	48 hrs	0.408	0.409	0.410	0.411	0.412	0.392

Table 4-4-7 Readings of UV-Spectrophotometer for Drug Release

Drug Release profile of the Eugarit E100 coated Nanoparticles pattern shows linear release of drug at pH 7.4. Initially absorbance values were 0.127 that increased to 0.408 with time. It is governed by dissolution and diffusion controlled mechanism. Eudagrit E 100 erodes with time which affects particle size ad parameter, then permeation of the fluid degrades the polymer which allows the drug encapsulated inside the polymer to diffuse outside polymeric nanoparticles. The After 24 hours of release value of absorbance decreased to 0.354 which indicates that maximum amount of drug was released at 24 hours. Lowered values of absorbance are due to low release and dilution. Dilution is caused as the result of the replacement of the sample with plain buffer solution. Drug content in each sample collected at different time interval was evaluated by using following formula:

$y = 0.236x + 0.0091$

$x = y - 0.0091 / 0.236$

Where,

y = Absorbance mean

x = drug content

Sample Code	Drug content (x) mg	Mean Absorbance (y)
A	3.9	0.128
B	4.03	0.193
C	3.89	0.202
D	4.04	0.210
E	4.10	0.295
F	4.12	0.322
G	4.13	0.354
H	4.5	0.392

Table 4-4-8 Readings of UV-Spectrophotometer for Drug content

In order to implement the kinetics model it is it is assumed that molecules of MTX migrated from region of higher concentration to the lower concentration until equilibrium is achieved,

concentration gradient remain linear with diffusion rate across the shell. According to fick's law it can be mathematically represented as:

$$dQ/dt = DAKm/w(C_{GIT} - C)/h$$

Where dQ/dt = drug diffusion per time

D is the diffusion coefficient its uit is m2/s (area/time),

A is the surface area for absorbing membrane for drug diffusion (area),

Km/w Partition coefficient

C_{GIT}- concentration of drug in buffer solution

C is concentration in plasma

$(C_{GIT} - C)$ is concentration gradient (amount per volume

h is membrane thickness

4.9.3 Application of kinetics models

Dissolution controlled drug release mechanism is followed by drugs that are encapsulated in polymer. In order to determine kinetics of the drug release different models such as zero order, first order, Higuchi, Hixen Crowell and korsemeyer Peppas models. Best fit model has been chosen on the basis of correlation coefficient (R^2). R-squared is a statistical measure of how close the data points are from regression line. It is also known as the coefficient of determination. Model with highest values indicates best fit to the release data. Given below is the table of all mathematical values required according to below defined models.

Time (Hr)	cumulative % drug released	% drug remaining	Square root time	log Cumu % drug remaining	log time	log Cumu % drug released	% Drug released	Cube Root of % drug Remaining(Wt)	Wo-Wt
0.5	78	22	0.707	1.342	0.000	0.000	100	2.802	1.840
1	80.6	19.4	1.000	1.288	0.000	1.906	2.6	2.687	1.955
2	77.8	22.2	1.414	1.346	0.301	1.891	-2.8	2.811	1.831
4	80.8	19.2	2.000	1.283	0.602	1.907	3	2.678	1.964
8	82	18	2.828	1.255	0.903	1.914	1.2	2.621	2.021
12	82.4	17.6	3.464	1.246	1.079	1.916	0.4	2.601	2.041
24	82.6	17.4	4.899	1.241	1.380	1.917	0.2	2.591	2.051
48	90	10	6.928	1.000	1.681	1.954	7.4	2.154	2.488

Table 4-9Mathematical calculation of kinetics models

Following are the list of the models that have been employed:

1. Zero order model
2. First order kinetics model
3. Hixon-Crowell
4. Higuchi
5. Korsemeyer – Peppas

4.9.3.1 Zero order models:

This model assumes a linear release of the drug into the buffer solution. Its graph is generated between time and cumulative drug release.

$Q_t = Q_0 + K_0 t$

Q_t cumulatative amount of drug released at time t,

Q_0 is the initial concentration of drug at time t=0,

K_0 is the zero-order rate constant.

Zero-Order Kinetics

y = 0.2185x + 79.057
R² = 0.8835

Fig 4.23 Graph for zero-order model

4.9.3.2 First order kinetics model:

Release is dependent on the concentration in first order reaction which indicates that if concentration is more than reaction is faster and vice versa. Its graph is generated between time and log percent of remaining cumulative drug release. It is mathematically represented as:

$\log Qt = \log Qo + kt/2.303$

where,

k is constant
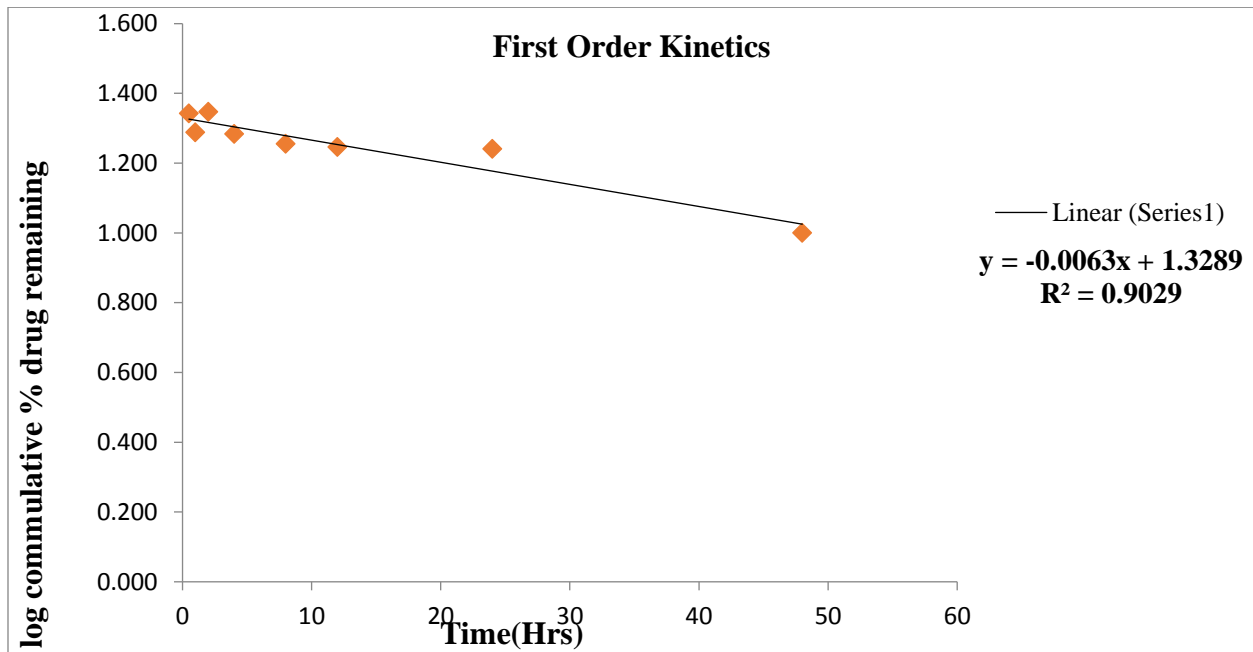
Fig 4.24 Graph for first order model

4.9.3.3 Hixon-Crowell:

Cube root Hixon Crowell model law is employed for the particles that have linear change in diameter. Hence the particles with regular area are directly proportional to the volume. Its graph is generated between cube root of remaining drug percentage and time. It is mathematically represented as:

$W_0{}^{1/3} - W_t{}^{1/3} = kt$

W_0 is initial amount of drug.

W_t is remaining amount of drug.
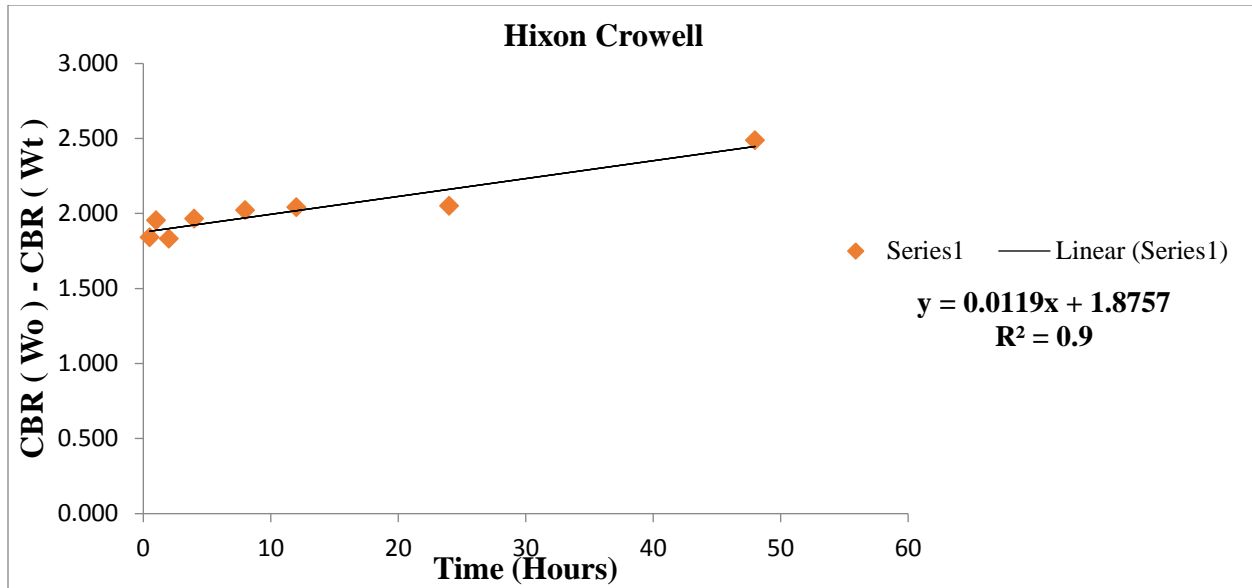
Fig 4.25 Graph for Hixon Crowell model

4.9.3.4 Higuchi

It's dependent on both diffusion and dissolution, since dissolution is important phenomenon in controlled drug release due to which this model is widely employed in controlled drug release system. Its graph is generated between square root of time and cumulative percentage drug release. It is mathematically represented as:

$Q = k_h \, t^{\frac{1}{2}}$ where K_h is Higuchi dissolution constant
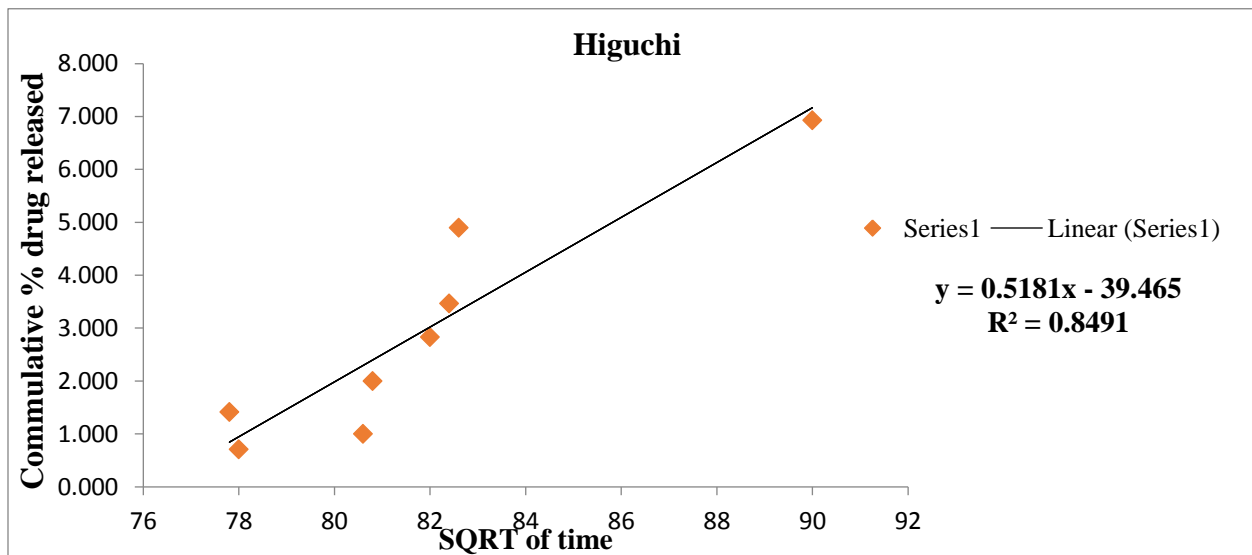
Fig 4.26 Graph for Higuchi model

4.9.3.5 Korsemeyer – Peppas

once it is found out by higuchi that druf release is following diffusion then korsemeyer – peppas model is employed to find which itype of dissolution by finding its its exponent value n. it is a simple mathematical equation which depicts which drug release from polymer shell into buffer solution. Its graph is generated between square root of time and cumulative percentage drug release. It is mathematically represented as:

$F = (M_t - M) = k_m t^n$

Where,

Fraction of dug at time t

M_t is amount of drug release at time t

M is total amount of drug

k_m is kinetic constant

n is release diffusion constant
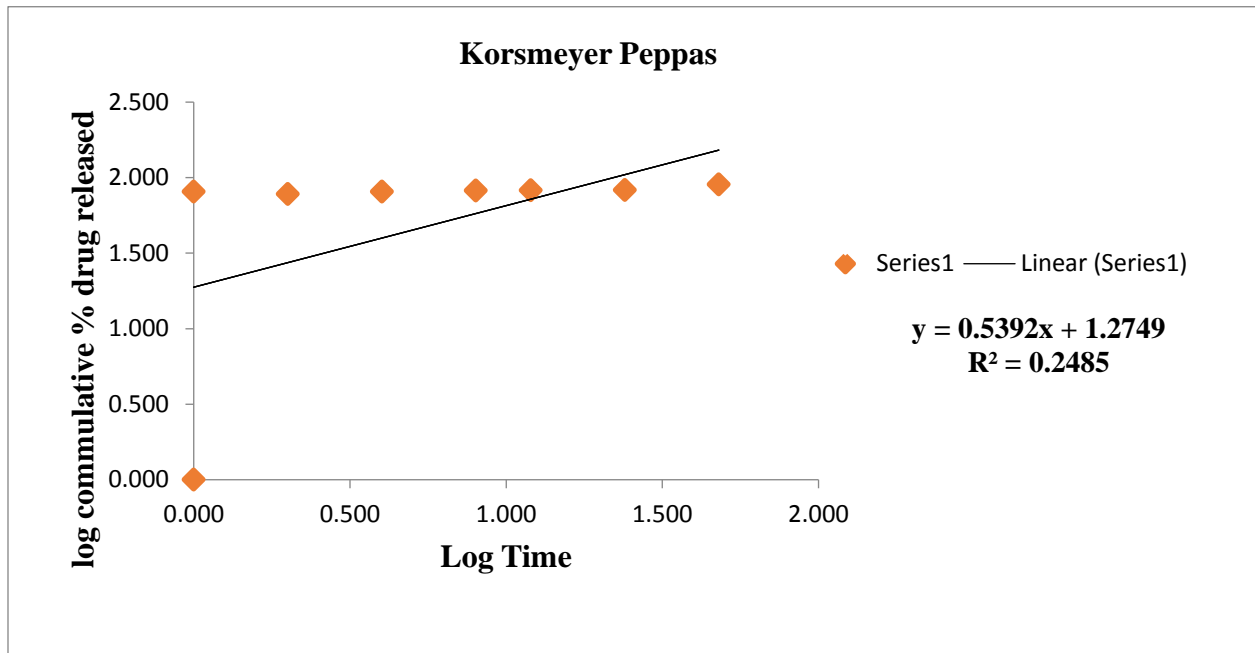
Fig 4.27 Graph for korsemeyer – peppas model

4.9.3.6 Analysis:

Highest values were achieved for Hixson Crowell and first order drug release models. Hixson Crowell model is used for the particles that have linear change in diameter. Hence the particles with regular area are directly proportional to the volume. In the presence of external stimuli i.e. change in pH polymeric shell of Eudagrit E 10 starts to erode which results in the change in the surface area of the nanoparticles. Erosion of polymeric shell is further accelerated by permeation of the fluids which results in the diffusion of drug particles. Dissolution was observed for up to 48 hours for nanoparticles of iron cobalt coated eudagrit e 100 polymers which corresponds to 90 % drug release. Below is the table that shows R^2 values for all the models that have been employed.

Factor	Zero order	First order	Higuchi	Hixson	Korse - Peppas
R^2	0.838	0.902	0.849	0.900	0.247

Table 4-10 R^2 of of kinetics model

Conclusions and Recommendations

Currently polymeric magnetic colloid is an area of research due to huge potential in the field biomedical. Over the past few a large amount of papers has been published which proves wide heritage for the development of nano-scientific research. Magnetically responsive polymer colloids have been prepared that opens door to the new regime of research platforms. Methotrexate loaded pH sensitive magnetic nanoparticles has been successfully developed through single emulsion solvent evaporation method in which ethanol was evaporated. Vibrating sample magnetometer, scanning electron microscope and XRD was carried out for $CoFe_2O_4$ nanoferrites and magnetization of 23nm sized particles was 1564 G. XRD peaks were successfully matched with data available in literature review; similarly zeta potential was carried out to find sizes and +8.96 mV of charge around colloids. Likewise positive results in terms of in vitro drug release profile were obtained that shows successful coating of eudagrit E100 around magnetic nanoparticles. Magnetically responsive $CoFe_2O_4$ nanoferrites for theranostic applications were investigated by various parameters studies on their stability and performance. Dissolution for drug release study was observed for up to 48 hours for nanoparticles of iron cobalt coated eudagrit E100 polymers which corresponds to 90% drug release. Drug release capability in accordance to kinetic models was also investigated and R^2 was determined. R^2 values of 0.902 were achieved for Hixson Crowell which indicates that it is best fit model. MTX loaded heat sensitive magnetic nanoparticles can be progressively used as successful strategy for the cancer and overcome many obstacles in the way of targeting only effected tissues. However more efforts are required to bring this study on higher scale and investigate its effects on animals and cell culture models.

References

[1] American cancer society. http://www.cancer.org/2014

[2] Y. Barenholz, Doxil(R), the first FDA-approved nano-drug: lessons learned, J.Control. Release 160 (2) (2012) 117–134.

[3] S. Cecco, M. Aliberti, P. Baldo, E. Giacomin, R. Leone, Safety and efficacy evaluation of albumin-bound paclitaxel, Expert Opin. Drug Saf. 13(4) (2014) 511–520.

[4] C. Oerlemans, W. Bult, M. Bos, G. Storm, J.F. Nijsen, W.E. Hennink, Polymeric micelles in anticancer therapy: targeting, imaging and triggered release, Pharm. Res. 27 (12) (2010) 2569–2589.

[5] Xie J, Lee S, Chen X. Nanoparticle-based theranostic agents. Advanced Drug Delivery Reviews; 62(11) (2010)1064-79

[6] T. Lammers, F. Kiessling, W.E. Hennink, G. Storm, Nanotheranostics and image guided drug delivery: current concepts and future directions, Mol. Pharm. 7 (6) (2010) 1899–1912.

[7] X. S. Niu, W. P. Du, W. M. Du, Sens. Actuators B 99 (2004) 405.

[8] H.J. Nam, T. Sasaki, and N. Koshizaki, J. Phys. photo conductive materials Chem. B 110 (2006) 23081.

[9] P.S. Patil, L.D. Kadam, and C.D. Lokhande, Thin Solid Films 29 (1996) 272.

[10] K.J. Kim and Y.R. Park, Solid State Comm. 25 (2003)127.

[11] S. K. Park, T. Ishikawa, and Y. Tokura, Phys. Rev. B 58 (1998) 3717.

[12] The formation f the doxorubicin loaded targeted nanoparticles using nano precipitation, double emulsion and single emulsion for cancer treatment, Journal of nano medicine and nano technology Jibowu, J Nanomed nanotechnol (2016), 3-7.

[13] Z. Fan, P.P. Fu, H. Yu, P.C. Ray, Theranostic nanomedicine for cancer detection and Treatment, Yao Wu Shi Pin. Fen. Xi. 22 (1) ,(2014) 3–17.

[14] Aniket S. Wadajkara, Jyothi U. Menona,Tejaswi Kadapurea, , and Kytai T. Nguyena Design and Application of Magnetic-Based Theranostic Nanoparticle Systems Recent Patents on Biomedical Engineering, (2013), 6, 47-57

[15] Sun C, Fang C, Stephen Z, Veiseh O, Hansen S, Lee D, et al. Tumor-targeted drug delivery and MRI contrast enhancement bychlorotoxin-conjugated iron oxide nanoparticles. Nanomedicine(London, England). 2008 Aug; 3(4): 495-505.

[16] Yu MK, Jeong YY, Park J, Park S, Kim JW, Min JJ, et al. Drug-Loaded Superparamagnetic Iron Oxide Nanoparticles for Combined Cancer Imaging and Therapy In Vivo. Angewandte Chemie International Edition. 2008; 47(29): 5362-5.

[17] Multifunctional Solid Lipid Nanoparticles: a targeted approach for Rheumatoid Arthritis with theranostic applications João Albuquerque, Catarina Costa Moura, Bruno Sarmento, Salette Reis

[18] Michele K. Lima-Tenórioa,b, Edgardo A. Gómez Pinedab, Nasir M. Ahmadc, Hatem Fessi a, Abdelhamid Elaissari Magnetic nanoparticles: In vivo cancer diagnosis and therapy, international journal of pharmaceutics 493 (2015) 313-327

[19] Nathalie Schleich, Fabienne Danhier 1, Véronique Préat, Iron oxide-loaded nanotheranostics: Major obstacles to in vivo studies and clinical translation, Journal of Controlled Release 198 (2015) 35–54.

[20] L.Y. Rizzo, B. Theek, G. Storm, F. Kiessling, T. Lammers, Recent progress in nanomedicine: therapeutic, diagnostic and theranostic applications, Curr. Opin. Biotechnol. 24 (6) (2013) 1159–1166.

[21] Dolmans DE, Fukumura D, Jain RK. Photodynamic therapy for cancer. Nat Rev Cancer. (2003); 3: 380-387.

[22] Wang C, Tao H, Cheng L, Liu Z. Near-infrared light induced in vivo photodynamic therapy of cancer based on upconversion nanoparticles. Biomaterials. (2011); 32: 6145-6154.

[23] Zhou A, Wei Y, Wu B, Chen Q, Xing D. Pyropheophorbide A and c(RGDyK)Comodified Chitosan-Wrapped Upconversion Nanoparticle for TargetedNear-Infrared Photodynamic Therapy. Mol Pharm. (2012); 9: 1580-1589. 28. Zhao Z, et al. Multifunctional core-shell upconverting nanoparticles forimaging and photodynamic therapy of liver cancer cells. Chem Asian J. (2012); 7: 830-837.

[24] Zhao Z, et al. Multifunctional core-shell upconverting nanoparticles for imaging and photodynamic therapy of liver cancer cells. Chem Asian J. (2012); 7: 830-837.

[25] Liu K, et al. Covalently Assembled NIR Nanoplatform for Simultaneous Fluorescence Imaging and Photodynamic Therapy of Cancer Cells. ACS Nano.(2012)

[26] Chen R, Zhang L, Gao J, et al. Chemiluminescent nanomicelles for imaging hydrogen peroxide and self-therapy in photodynamic therapy. J Biomed Biotechnol. (2011); 679-492.

[27] Choi Y, et al. Highly Biocompatible Carbon Nanodots for Simultaneous Bioimaging and Targeted Photodynamic Therapy In Vitro and In Vivo. Advanced Functional Materials. (2014); 24(37): 5781-5789. 2743

[28] Tian G, et al. Red-Emitting Upconverting Nanoparticles for Photodynamic Therapy in Cancer Cells Under Near-Infrared Excitation. Small. (2013); 9(11): 1929-1938.

[29] [28] Cui S, et al. In Vivo Targeted Deep-Tissue Photodynamic Therapy Based on Near-Infrared Light Triggered Upconversion Nanoconstruct. ACS Nano. 2013; 7(1): 676-688.

[30] Zhang L, et al. Inorganic photosensitizer coupled Gd-based upconversion luminescent nanocomposites for in vivo magnetic resonance imaging and near-infrared-responsive photodynamic therapy in cancers. Biomaterials. (2015); 44: 82-90.

[31] Park YI, et al. Theranostic Probe Based on Lanthanide-Doped Nanoparticles for Simultaneous In Vivo Dual-Modal Imaging and Photodynamic Therapy. Advanced Materials. (2012); 24: 5755-5761.

[32] Idris NM, et al. In vivo photodynamic therapy using upconversion nanoparticles as remote-controlled nanotransducers. Nature Medicine. (2012); 73-90.

[33] 18(10): 1580-1585. 32 36Rai P, et al. Development and Applications of Photo-triggered Theranostic Agents. Adv Drug Deliv Rev. (2010); 62(11): 1094-1124.

[34] Lindner U, Weersink RA, Haider MA, et al. Image guided photothermal focal therapy for localized prostate cancer: phase I trial. J Urol.(2009); 182: 1371-1377.

[35] Kost J, Leong K, Langer R. Ultrasound-enhanced polymer degradation and release of incorporated substances. Proc Natl Acad Sci U S A. (1989); 86: 7663-7666.

[36] Ferrara KW. Driving delivery vehicles with ultrasound. Adv Drug Deliv Rev. (2008); 60: 1097-1102.

[37] Simon DT, et al. Organic electronics for precise delivery of neurotransmitters to modulate mammalian sensory function. Nat Mater. (2009); 8: 742-746. 37120

Moscicka-Studzinska A, Czarnecka K, Ciach T. Electrically enhanced and controlled drug delivery through buccal mucosa. Acta Pol Pharm. (2008); 65: 767-769.

[38] Svirskis D, Travas-Sejdic J, Rodgers A, Garg S. Electrochemically controlled drug delivery based on intrinsically conducting polymers. J Control Release. (2010); 146: 6-15.

[39] Elsherbini AA, Saber M, Aggag M, et al. Laser and radiofrequency-induced hyperthermia treatment via gold-coated magnetic nanocomposites. Int J Nanomedicine. (2011); 6: 2155-2165.

[40] Alexandra Sneider, Derek VanDyke, Shailee Paliwal, Prakash Rai, Remotely Triggered Nano Theranostics For Cancer Applications, 2017; 1(1): 1-22. doi: 10.7150/ntno.17109.

[41] Surface-Modified Superparamagnetic Nanoparticlesfor Drug Delivery: Preparation, characterization, and cytotoxicity studiesajay kumar gupta* and stephen wells IEEE transactions on nanobioscience, vol. 3, no. 1, march (2004) page 66-73

[42] C. Chouly, D. Pouliquen, I. Lucet, J. J. Jeune, and P. Jallet, "Development of superparamagentic nanoparticles for MRI: Effect of particle size, charge and surface nature on biodistribution," J. Microencapsulation,vol. 3, pp. 245–255, 1996.

[43] S. Stolnik, L. Illum, and S. S. Davis, "Long circulating microparticulate drug carriers," Adv. Drug Delivery Rev., vol. 16, pp. 195–214, 1995.

[44] Oil/water Nano-emulsion loaded with cobalt ferrite oxide nanocubes for photo-acoustic and magnetic resonance dual imaging in cancer: in vitro and preclinical studies Nano medicine: Nanotechnology, Biology, and Medicine, 13 (2017) 275–286

[45] Gaumet M, Vargas A, Gurny R, Delie F. Nanoparticles for drug delivery: the need for precision in reporting particle size parameters. Pharm Biopharm (2008) ;69:1

[46] Papis E, Gornati R, Prati M, Ponti J, Sabbioni E, Bernardini G. Gene expression in nanotoxicology research: analysis by differential display in BALB3T3 fibroblasts exposed to cobalt particles and ions. Toxicol Lett (2007);107:185-92.

[47] Monodisperse mesoporous cobalt ferrite nanoparticles: synthesis and application in targeted delivery of antitumor drugs DOI: 10.1039/c1jm10732a

[48] Synthesis and characterization Z. Karimi , S. Abbasi , H. Shokrollahi , Gh. Yousefi , Materials Science and Engineering C 71 (2017) 504–511.

[49] Structural phase stability and Magnetism in Co_2FeO_4 spinel oxide. Panneer Muthuselvam and R.N. Bhowmik*Department of Physics, Pondicherry University, R. Venkataraman Nagar,Kalapet, Pondicherry-605014, India

[50] Optimization of Magnetic Properties in Cobalt Ferrite Nanocrystals Y. Cedeño-Mattei, O. Perales-Pérez, M. S. Tomar and F. Román University of Puerto Rico, Mayagüez, PR 00681-9044.

[51] Muhammad A. Hassan1, Mudassara Saqib, Haseeb Shaikh1, Nasir M. Ahmad and Abdelhamid Elaissari, Magnetically Engineered Smart Thin Films: Toward Lab-on-Chip Ultra-Sensitive Molecular Imaging, Journal of Biomedical Nanotechnology Vol. 9, (2013) 467–474,

[52] In vitro MRI of biodegradable hybrid (iron oxide/polycaprolactone) magnetic nanoparticles prepared via modified double emulsionevaporation mechanismNaveed Ahmeda, Nasir M. Ahmad, Hatem Fessic, Abdelhamid Elaissaric,∗] Colloids and Surfaces B: Biointerfaces 130 (2015) 264–271

[53] Nadia Naseer1, Hira Fatima2, Arfa Asghar1, Nosheen Fatima2, Naveed Ahmed, Magnetically Responsive Hybrid Polymer Colloids for Ultrasensitive Molecular Imaging, Journal of Colloid Science and Biotechnology (2014) Vol. 3, 1–11,

[54] Michele K. Lima-Tenórioa,b, Edgardo A.Gómez Pinedab, Nasir M. Ahmad, Aminodextran polymer-functionalized reactive magnetic emulsionsfor potential theranostic applications, Colloids and Surfaces B: Biointerfaces, Colloids and Surfaces B:

[55] B. D. Culity, C. D. Graham Introduction to Magnetic Materials (2009): Wiely-Interscience.

[56] SRM university lectures

[57] Raffaele Vecchione, Vincenzo Quagliariello,Pierangela Giustetto,Oil/water nano-emulsion loaded with cobalt ferrite oxide nanocubes for photo-acoustic and magnetic resonance dual imaging in cancer: in vitro and preclinical studies, Nanomedicine: Nanotechnology, Biology, and Medicine 13 (2017) 275–286. Synthesis and characterization Z. karimi, S.Abbasi, Gh. Yousefi, Material Science and Engineering 71(2017) 504-511.

[58] Miladi, K., Ibraheem, D., Iqbal, M., Sfar, S., Fessi, H., Elaissari, A., 2014. Particles frompreformed polymers as carriers for drug delivery. EXCLI J. 13, 28–57.

[59] S. Foner "Versatile and Sensitive Vibrating Sample Magnetometer" Rev. Sci. Instrum, 30(1959)548.

[60] Debi Prasad Pattnaik.Design and Fabrication of Vibrating Sample Magnetometer Thesis. Department of Physics and Astronomy. National Institute of Technology Rourkela, Odisha, India.

[61] B. R.Kirupakar*1, Dr.B.A.Vishwanath, M. Padma Sree, Deenadayalan, Vibrating Sample Magnetometer and Its Application In Characterization Of Magnetic Property Of The Anti-Cancer Drug Magnetic Microspheres review article, Aditya Bangalore Institute Of Pharmaceutical Education And Research, Rajiv Gandhi University Of Health Sciences, Karnataka, WuShiZuo, PengJinHua; LiFengSheng. Preparation and Characterization Fluorescent Magnetic Target Drug Delivery System. PhD thesis. Nanjing University of Technology and Engineering. 2012. Accessed on 06 March (2016).

[62] Goldstein, G. I.; Newbury, D. E.; Echlin, P.; Joy, D. C.; Fiori, C.; Lifshin, E. (1981). Scanning electron microscopy and x-ray microanalysis. New York: Plenum Press. ISBN 0-306-40768-X.

[63] Y. Cedeño-Mattei, O. Perales-Pérez*, M. S. Tomar and F. Román Optimization of Magnetic Properties in Cobalt Ferrite Nanocrystals, ENS'07 Paris, (December 2007) France, 3-4

[64] Sasmita Mohapatra,*a Smruti R. Rout,a Swatilekha Maiti,b Monodisperse mesoporous cobalt ferrite nanoparticles: synthesis and application in targeted delivery of antitumor drugs, Journal of Dynamic Article , Materials Chemistry, 15th April 2011, J. Mater. Chem., (2011), 21, 9185

[65] Din FU, Mustapha O, Rashid R, Kim DW, Park JH, Ku SK, Oh YK, Kim JO, Youn YS, Yong CS, Choi HG. Novel dual-reverse thermosensitive solid lipid nanoparticle-loaded hydrogel for rectal administration of flurbiprofen with improved bioavailability and reduced initial burst effect. European Journal of Pharmaceutics and Biopharmaceutics. (94) 64-72, 2015a.

[66] Din FU, Rashid R, Mustapha O, Kim DW, Park JH, Ku SK, Kim JO, Youn YS, Yong CS, Choi HG. Development of a novel solid lipid nanoparticles loaded dual-reverse thermosensitive nanomicelle for intramuscular administration with sustained release and reduced toxicity. RSC Advances(5) 43687-43694 2015b.

[67] Din FU, Ju Yeon Choi, Dong Wuk Kim, Mustapha O, Kim DW, Kim DS, Ku SK, Oh YK, Kim JO, Yong CS, Choi HG. Irinotecan-encapsulated double-reverse thermosensitive nanocarrier system for rectal administration. 24(1): 502–510. Drug Delivery 2017a.

[68] Din FU, Dong Wuk Kim, Ju Yeon Choi, Mustapha O, Kim DW, Kim DS, Thapa RJ, KT OH, Ku SK, Kim JO, Youn YS, Yong CS, Choi HG. Irinotecan-loaded double-reversible thermogel with improved antitumor efficacy without initial burst effect and toxicity for intramuscular administration. Acta Biomaterelia 54 (2017b) 239–248.

[69] Langer R. New methods of drug delivery. Science. 1990; 249:1527–1533. [PubMed]